iScience

CellPress
OPEN ACCESS

Article

M-*O*-M mediated denaturation resistant P2 tetramer on the infected erythrocyte surface of malaria parasite imports serum fatty acids

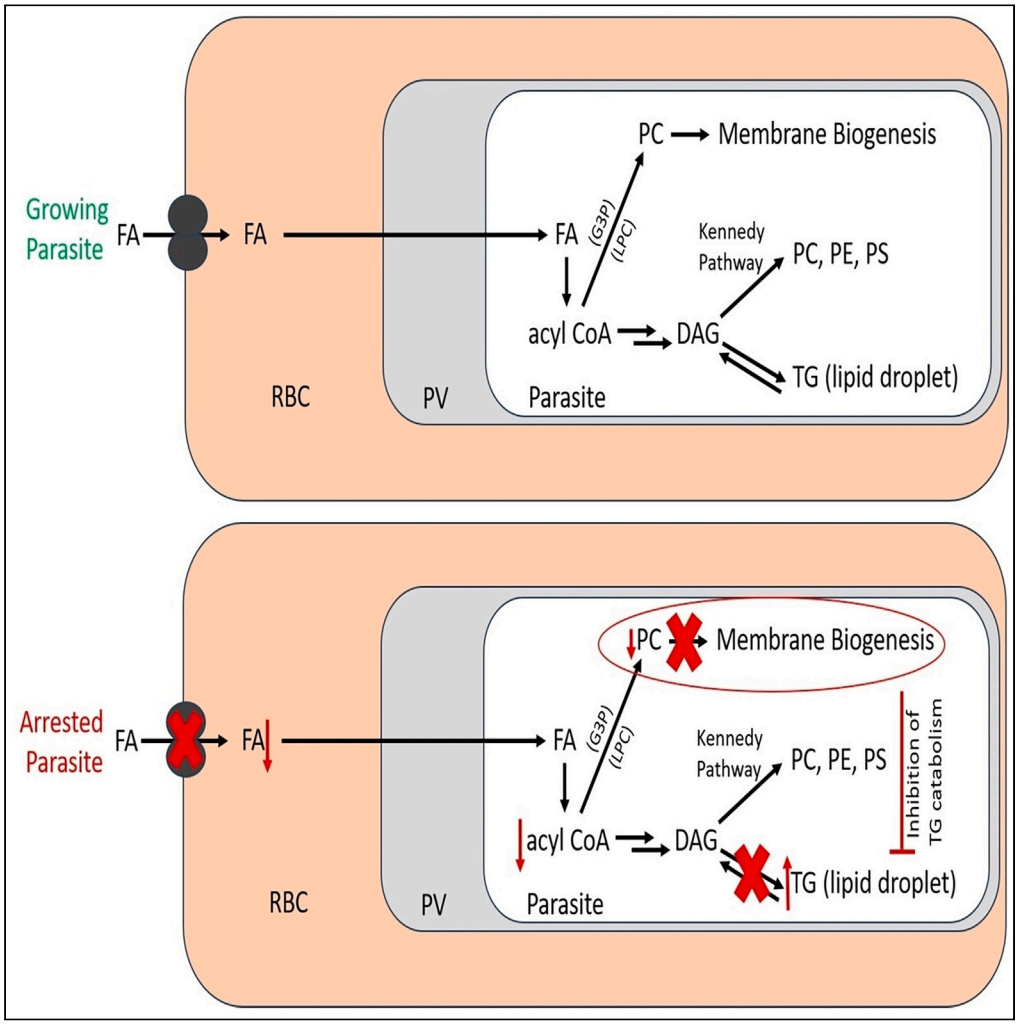

Sudipta Das, Anwesa Manna, Oindrila Majumdar, Lena Dhara

sudipta.das@iicb.res.in

Highlights

Denaturation-resistant PfP2 tetramers on the IE surface import fatty acids (FAs)

Inhibition of serum FAs import led to the reversible arrest of schizogony

Denaturation resistance is due to Methionine 11 oxidation among four PfP2 monomers

$^{12/53}$Cys-Cys$^{12/53}$ redox switch in PfP2 tetramer regulates FAs binding and release

Das et al., iScience *27*, 109760
May 17, 2024
https://doi.org/10.1016/j.isci.2024.109760

iScience

CellPress
OPEN ACCESS

Article

M-*O*-M mediated denaturation resistant P2 tetramer on the infected erythrocyte surface of malaria parasite imports serum fatty acids

Sudipta Das,[1,4,*] Anwesa Manna,[2,3] Oindrila Majumdar,[2,3] and Lena Dhara[2]

SUMMARY

In *Plasmodium falciparum*, DNA replication, and asynchronous nuclear divisions precede cytokinesis during intraerythrocytic schizogony. Regulation of nuclear division through the import of serum components was largely unknown. At the trophozoite stage, *P. falciparum* ribosomal protein P2 (PfP2) is exported to the infected erythrocyte (IE) cytosol and the surface as a denaturation-resistant tetramer. The inaccessibility of the IE surface exposed PfP2 to its bona fide ligand led to the arrest of nuclear division. Here, we show that at the onset of schizogony, denaturation-resistant PfP2 tetramer on the IE surface imports fatty acids (FAs). Blockage of import reversibly arrested parasite schizogony. In ^{11}Met-*O*-Met^{11} mediated denaturation resistant PfP2 tetramer, the $^{12/53}$Cys-Cys$^{12/53}$ redox switch regulates the binding and release of FAs based on oxidized/reduced state of disulfide linkages. This mechanistic insight of FAs import through PfP2 tetramer reveals a unique regulation of nuclear division at the onset of schizogony.

INTRODUCTION

Plasmodium falciparum (*P. falciparum*), the causative agent of malaria, remains a huge public health burden globally.[1] During intraerythrocytic schizogony, *P. falciparum* shows repeated asynchronous nuclear division giving rise to 16–32 daughter parasites called merozoite.[2–11] In addition to protozoan parasites, nuclear asynchrony has also been observed in fungi.[12] In *P. falciparum*, how the asynchrony is being achieved and maintained is not clear. In order to commit for repeated DNA replication and nuclear division, *P. falciparum* needs to ensure optimum supply of required nutrients.[4,6,10,13] FAs and lipids are important nutrients necessary for membrane biogenesis to sustain ongoing nuclear division and merozoite formation.[14] Deprivation of nutrients prevents cell cycle initiation at the G1/S checkpoint in mammalian cells.[15] It is not yet known whether in *P. falciparum,* the deprived levels of lipids/nutrients have any role to play in triggering asynchronous cell-cycle arrest. Asynchronous nuclear division has been speculated to be due to the local skewing of nutrients or might be due to limiting factors that slow down the multiplication of nuclei as it progresses toward mature schizogony.[5–11] During repeated asynchronous nuclear division, DNA content of individual nucleus doubles after replication followed by mitosis (S/M Phase) mediated by microtubules and this process repeats several times before merozoite formation.[10,11] During S/M Phase in *P. falciparum*, polymerization and depolymerization of microtubules play a pivotal role, however the structures of microtubule during ongoing nuclear division do not look homogeneous and that might be one of the reasons for nuclear asynchrony during schizogonic cell division.[10,13] Some recent reports indicate that at the onset of nuclear division or before the full commitment for S/M phase, checking the level of sufficient nutrients is critically important.[10,11,13,16] The nutrient level mediated cell cycle regulations and its molecular nature are largely unknown in *P. falciparum*. However, similarities, with the mammalian G1/S checkpoint (restriction point) or START point in yeast can be noted.

During the IE development of *P. falciparum*, nuclear division precedes membrane biogenesis and progeny merozoite formation.[17–21] Hence abrogation in the process of lipid biosynthesis due to altered levels of FAs, diglycerides (DG), and triglycerides (TG), might convey a negative signal to the process of nuclear division in general and as a result, parasite proliferation may be reversibly halted until FA, DG, and TG reaches its normal level required to resume lipid biosynthesis and membrane biogenesis. During the trophozoite stage, the lipid content of the parasite increases by 200%–300% through the acquisition and biosynthesis of a large number of lipid species.[17,18] Phospholipids (PL) are the major structural element of the parasite membranes and phosphatidylcholine (PC) is the most abundant PL in the parasite membrane during blood stage development.[19–21] The parasite possesses a *de novo* PL biosynthesis pathway to generate (lyso)PL classes and their precursors from FAs through the Kennedy pathway and the cytidine diphosphate-diacylglycerol (CDPDAG) pathway.[18,19] Hence, a steady source of FAs must be channelized for PL biosynthesis during parasite nuclear division and membrane biogenesis. During the IE stage of *P. falciparum*, there is no *de novo* biosynthesis of FAs,[14] hence for membrane PL biosynthesis, FAs must be scavenged from the host lipid

[1]Division of infectious Disease and Immunology, CSIR-Indian Institute of Chemical Biology, 4, Raja S.C Mullick Road, Jadavpur, Kolkata 700032, India
[2]Division of infectious Disease and Immunology, CSIR-Indian Institute of Chemical Biology, 4, Raja S.C Mullick Road, Jadavpur, Kolkata 700032, India
[3]These authors contributed equally
[4]Lead contact
*Correspondence: sudipta.das@iicb.res.in
https://doi.org/10.1016/j.isci.2024.109760

milieu or imported from the human serum. Till date, there are no reports which describes the mechanism how FAs get imported into the parasite either from the host milieu or from the serum. The transport of long-chain FAs across the cell membrane has long been thought to occur by passive diffusion. However, in recent years there has been a fundamental shift in understanding, and it is now generally accepted that FAs cross the cell membrane via a protein mediated mechanism. Membrane associated FA-binding proteins ('FA transporters') not only facilitate but also regulate cellular FAs uptake.[22,23]

The gene expression of 60S stalk ribosomal protein P2 (PfP2) (PF3D7_0309600) is independent of the developmentally regulated rRNAs.[24] PfP2 is a non-PEXEL (Plasmodium Export Element) protein. It has been reported to be present in the IE cytosol[25] and exposed out from the IE surface during the mid-late trophozoite stage.[26–28] Post-merozoite invasion (PMI) at around 30h, PfP2 was found to be present on the IE surface for around 8–9h as a denaturation resistant PfP2 tetramer.[26–28] According to the flow cytometric analysis, when IE surface exposed PfP2 was made inaccessible to its bona fide ligand(s) through anti-PfP2 monoclonal antibody (E2G12) binding, the nuclear division of the parasite was reversibly arrested at the onset of nuclear division.[26] With the continued presence of E2G12 in the culture medium, nuclear division did not progress as the MFI (Mean fluorescence Intensity) of DAPI stained parasites did not increase till 48h PMI, whereas MFI of DAPI stained control parasites enhanced significantly.[26] This suggested that continued blockage of PfP2 tetramer on the IE surface using monoclonal antibody did not allow parasite nuclear division to resume whereas in the absence of antibody, nuclear division proceeded and completed schizogony.[26] Selective removal of palmitic acid and oleic acid from the culture medium was also shown to inhibit nuclear division at the onset of parasite nuclear division, which indicates an essential role of serum FAs at the onset of parasite schizogony.[29–33] In the present study, we have uncovered the function of PfP2 tetramer on the IE surface and how it is possibly linked with the parasite nuclear division at the onset of schizogony. We have identified that the denaturation resistant PfP2 tetramer on the IE surface interacts and import serum FAs. Inhibition of FAs import resulted into TG accumulation possibly due to the inhibition of its catabolism and as a consequence the nuclear division of the parasite was reversibly halted. In the denaturation resistant PfP2 tetramer, we report that the 'S' atom of the 11th methionine residue in the PfP2 monomer was oxidized and as a result ^{11}Met-*O*-Met^{11} (M-*O*-M) covalent linkages were formed resulting in the formation of denaturation resistant PfP2 tetramer. In this resistant tetramer, the $^{12/53}$Cys-Cys$^{12/53}$ redox switch regulates the binding and subsequent release of FAs based on the oxidized/reduced state of disulfide linkages in the denaturation resistant PfP2 tetramer. Inhibition of FAs import through PfP2 tetramer on the IE surface resulted in the arrest of nuclear division may be due to the downstream TG accumulation and abrogation of membrane biogenesis. This arrest of the nuclear division was reversible upon FAs import through the PfP2 tetramer, hence appearing to have a link which seems to regulate parasite nuclear division at the onset of schizogony. This FAs import mediated reversible nature of nuclear division arrest and its recovery seem to indicate a checkpoint like phenomenon at the onset of parasite schizogony.

RESULTS

At the onset of nuclear division PfP2 tetramer localizes on the IE surface

At the mid-late trophozoite stage, PfP2 protein is trafficked to the IE surface.[26,27] Blocking the accessibility of IE surface exposed PfP2 using E2G12[26] or by genetic knockdown of PfP2 protein using pLN-glmS-ribozyme (PfP2-HA parasites) and glucosamine (GlcN) resulted in schizogony arrest of the parasites (Figures S1A–S1C). Absence/presence of 3 mM GlcN did not seem to have any physiological effect on the wild type Pf3D7 parasites as the parasitemia at different days were almost similar (Figure S1F). In the presence of 3mM GlcN, PfP2-HA transgenic parasites did develop from ring to trophozoite stage comparable to not GlcN treated (control) parasites (Figure S1C). At around 24h PMI, % trophozoites in the absence/presence of GlcN did not differ (Figure S1C). But PfP2-HA transgenic parasites did not progress through trophozoite to schizont stage when PfP2 was downregulated in the presence of 3 mM GlcN (Figure S1C). In the absence of GlcN, around 48h PMI control parasites completed their life cycle hence formed fresh rings but in the presence of GlcN, trophozoites remain arrested and did not proceed toward schizogony hence showed high percentage of trophozoite parasites at 48h PMI (Figure S1C and S1H). When GlcN was washed out to check whether arrested trophozoite stage parasites rescue and proceed toward schizogony, we observed around 70–80% multinucleated trophozoites with a varying degree of multinuclearity which indicated that the arrest was reversible to the significant population of the PfP2-HA transgenic parasites (Figures S1I and S1J). Around 80–90% PfP2-HA transgenic parasites showed the presence of PfP2 on the IE surface at trophozoite stage (Figures S1D and S1E). To understand the correlation between schizogony arrest and the localization of PfP2 on the IE surface, PfP2-HA transgenic parasites (Figure S1) were synchronized and at 18-22h PMI, taxol was added in parasite culture medium (Figure 1A). Taxol as a known inhibitor of tubulin depolymerization causes mitosis arrest by preventing chromosome segregation and daughter nuclei formation. However, in *P. falciparum* taxol does not define any window of cell cycle checkpoint but in the absence of any known cell cycle inhibitor, taxol appeared to us to be the best choice to induce mitosis arrest in *P. falciparum*.[34] After 6h of taxol treatment, mitosis arrested IEs at around 28-30h PMI were stained for the localization of PfP2, tubulin and the nucleus (Figures 1B and 1D). Immunofluorescence assay (IFA) using anti-HA antibody and confocal imaging of taxol arrested IEs distinctly showed the green punctate nature of PfP2 in every optical plane of an IE showing PfP2 on the IE surface and in the IE cytosol (Figures 1B and 1C). IFA also depicted the arrested nuclei and the status of tubulin in around 95% taxol induced mitosis arrested PfP2-HA transgenic parasites (Figures 1D–1F). Around 90–95% taxol arrested PfP2-HA transgenic parasites showed PfP2 on the IE surface (Figures 1C, 1D, and 1E) confirming its RBC surface localization. IFA of taxol arrested PfP2-HA transgenic parasites at trophozoite stage using E2G12[26] clearly showed IE surface and IE cytosol localization of PfP2 (green puncta) (Figure 1F). It is important to mention that as compared to our previous study,[26] we have observed a substantial increase in IE surface localized PfP2 when mitosis was arrested with taxol. Immunoblot of parasite lysate, IE ghost and IE cytosol of PfP2-HA transgenic parasites using E2G12 clearly showed the presence of PfP2 monomer (~15 kDa) and tetramer (~60 kDa) in the parasite lysate whereas in the IE ghost and cytosol predominantly tetramer species were observed (Figure 1G). Interestingly, at 28-30h PMI at the trophozoite stage, around

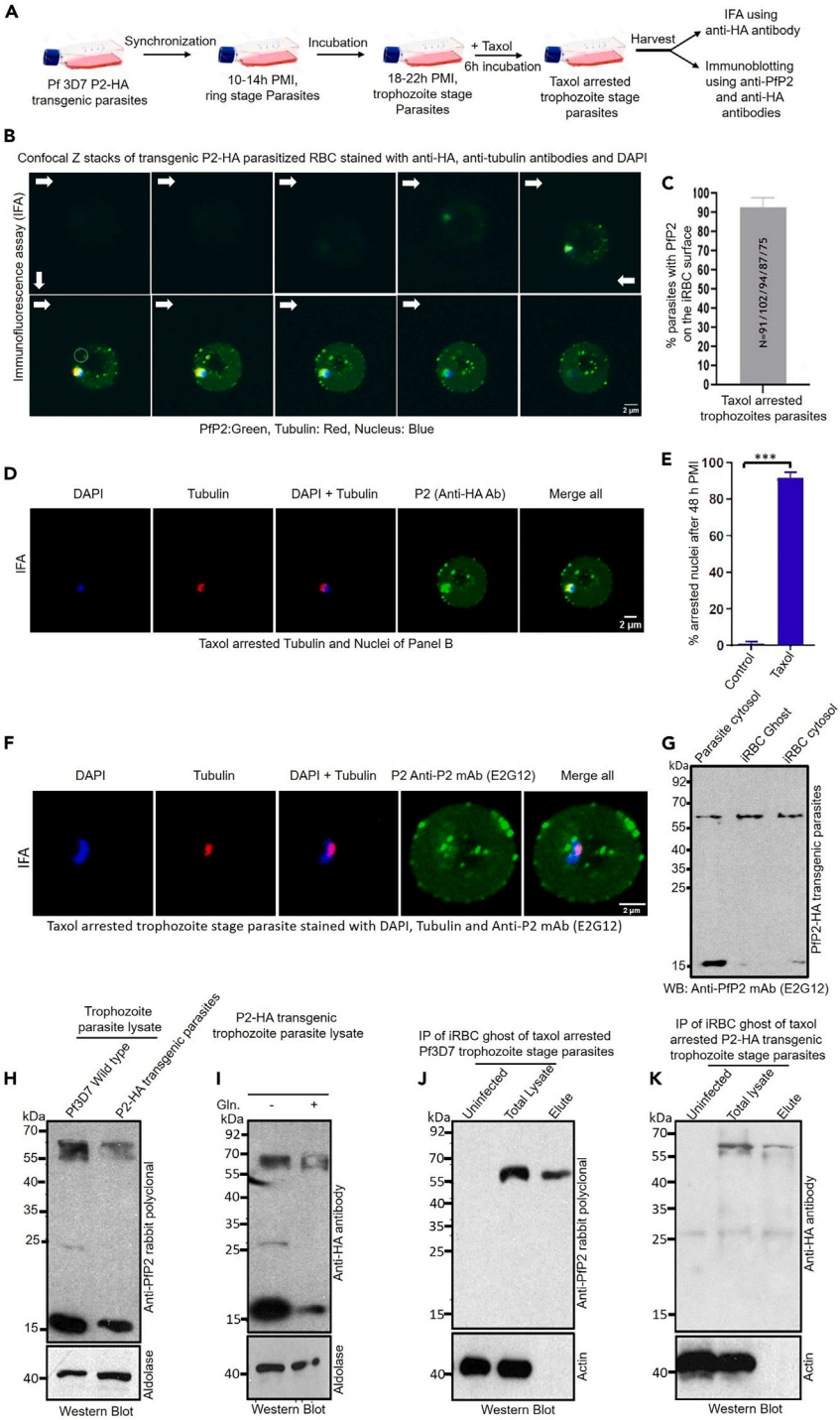

Figure 1. PfP2 tetramer localizes on the IE surface at the onset of parasite nuclear division

(A) Schematic depiction of the process of synchronization and taxol treatment of *P. falciparum* 3D7 P2-HA (PfP2-HA) transgenic parasites and subsequent usage of taxol-arrested parasites.

(B) Immunofluorescence assay (IFA) of taxol arrested PfP2-HA parasites followed by confocal optical sectioning through the z axis. Parasite P2 (green puncta) was stained with anti-HA antibody, and parasite tubulin (red) was stained with anti-β tubulin antibody. Parasite nuclei were stained with DAPI. The white arrow depicts the initiation of the optical slice and the subsequent revelation of parasite P2 protein (green puncta) at every z stack.

Figure 1. *Continued*

(C) Quantification of taxol arrested PfP2-HA transgenic parasites at trophozoite stage showing P2 protein on the infected RBC (IEs) surface. Five biological replicates of taxol treated parasites showed around 90–95% arrested nuclei at the trophozoite stage where PfP2 protein is present on the IE surface. ($N = 5$). Number represents the % arrested parasites showing PfP2 protein on the IE surface.

(D) Taxol arrested Panel B parasite showing the nuclei and the status of tubulin and the distribution of green punctate PfP2 throughout the infected RBC cytosol and the surface. PfP2-HA was stained by anti-HA antibody. Scale bar 2 μm.

(E) Percent arrested nuclei after 48h PMI with/without taxol treatment. $N = 3$.

(F) Taxol arrested PfP2-HA transgenic parasites at trophozoite stage stained with DAPI (blue), anti-tubulin antibody (red) and anti-PfP2 monoclonal antibody E2G12[26] (green). Scale bar 2 μm.

(G) Immunoblot of parasite lysate, IE ghost and IE cytosol of PfP2-HA transgenic parasites. The blot was probed with anti-PfP2 monoclonal antibody E2G12.[26]

(H) Immunoblot of wild type and transgenic PfP2-HA trophozoite stage parasites. Wild-type parasite lysate (2 μg) and PfP2-HA parasite lysate (2 μg) were separated in reducing SDS-PAGE and probed with anti-PfP2 rabbit serum. Parasite aldolase was used as a loading control.

(I) Immunoblot of transgenic trophozoite stage parasites in the absence/presence of GlcN (3 mM). Around 1.5 μg of parasite lysate was separated in reducing SDS-PAGE and probed with an anti-HA antibody. Parasite aldolase was used as a loading control.

(J) Immunoprecipitation (IP) of IE ghost of taxol arrested wild type parasites using anti-PfP2 rabbit polyclonal antibody. A total of 4 μg of IE ghost protein (Total Lysate/input) was incubated with 8 μg anti-PfP2 rabbit polyclonal antibody. IP material was separated in reducing SDS-PAGE and immunoblotted using anti-PfP2 antibody. As a control, uninfected RBC ghost total protein (4 μg) was used to check any antibody cross-reactivity. Ghost actin was used as a loading control.

(K) Immunoprecipitation (IP) of IE ghost of taxol arrested PfP2-HA transgenic parasites using anti-HA antibody. A total of 3 μg of IE ghost protein (Total Lysate/input) was incubated with 6 μg anti-HA immunoglobulin molecules. IP material was separated in reducing SDS-PAGE and immunoblotted using an anti-HA antibody. As a control, uninfected RBC ghost total protein (3 μg) was used to check any HA antibody cross-reactivity. Ghost actin was used as a loading control. N represents biological replicates. All quantitative experiments were repeated at least three times or more as indicated. Significance was considered at $*p < 0.05$, $**p < 0.01$, $***p < 0.001$.

85–90% of transgenic parasites showed PfP2-HA on the IE surface (Figures S1D and S1E) which hinted about a possible role of PfP2 on the IE surface at the onset of schizogony. The cytosol of wild-type and PfP2-HA transgenic parasites clearly showed two species of the protein, monomeric PfP2 (~15 kDa) and denaturation resistant PfP2 tetramer (~60 kDa) (Figure 1H). With 3 mM GlcN, when cytosolic PfP2-HA was downregulated, that resulted in the arrest of parasite schizogony (Figures 1I, S1B, and S1C). Immunoprecipitation (IP) of IE ghost from wild type and PfP2-HA transgenic parasites using PfP2 rabbit polyclonal and anti-HA antibody respectively revealed the presence of denaturation resistant PfP2 tetramer on the IE surface and in the IE cytosol (Figures 1J and 1K). These observations explicitly suggested a molecular event occurring in the cytosol of trophozoite stage parasites resulting in the formation of denaturation resistant PfP2 tetramer and subsequent trafficking to the IE surface.

In vitro generation of denaturation resistant PfP2 tetramer where Methionine oxidation and inter-peptide ^{Met11}S-*O*-S^{Met11} covalent linkages in PfP2 tetramer generates denaturation resistance

On the IE surface, PfP2 exists as a denaturation resistant tetramer which did not resolve to a monomer even after boiling in DTT treated SDS-PAGE.[26,28] It was difficult to acquire sufficiently pure IE ghost tetrameric PfP2 material required for subsequent biochemical and biophysical experimentations to fish out the reasons for denaturation resistance. Using a unique approach, *in vitro* we successfully synthesized denaturation resistant PfP2 tetramer involving incubation of 6x His tag recombinant PfP2 (rec. PfP2) with albumax (a parasite culture component rich in lipids and bovine serum proteins) or human serum. But rec. PfP2 was not incubated with complete albumax/serum, instead, albumax was dissolved in 1xPBS and then passed through a 5 kDa membrane cutoff filter which did not allow serum proteins in the passed-through solution. Hence, after cutoff filtration we used passed through (flow through) solution as we named lower albumax fraction solution (LAFS) which predominately possessed small molecules present in the albumax/serum and was mostly devoid of serum proteins (Figure S2A). When rec. PfP2 was incubated with LAFS at 37°C for 3h and resolved in nonreducing SDS-PAGE, all the species of rec. PfP2 (monomer and dimer), converted into a tetramer (Figure S2B). Whereas 6x His tag control proteins from mammalian and plant origins did not show any such transformation (Figure S2C), which suggested a ligand induced rec. PfP2 tetramer formation. We hypothesized that small molecule(s) of any nature present in LAFS has the potential to drive rec. PfP2 oligomerization into a tetramer. To understand the authenticity of this transformation, we simply titrated out small molecule(s) from LAFS by incubating rec. PfP2 with LAFS followed by affinity purification with Ni-NTA beads. During another incubation of fresh rec. PfP2 with one-time used LAFS, tetramerization was observed to be significantly diminished and predominantly monomer, dimer, and low level of tetramer were noticed (Figure S2D). This clearly suggested that in LAFS, the quantity of ligand(s) whatever it may be (possibly small molecules) was exhausted due to its first-time consumption by rec. PfP2. Hence during the second incubation, enough small molecule(s) were not available in LAFS for the second transformation to occur. To check whether LAFS-treated rec. PfP2 tetramer shows denaturation resistance like PfP2 tetramer in IE ghost,[26] we finally went ahead and checked the stability of LAFS-treated rec. PfP2 tetramer in 4M urea SDS-PAGE with boiling under reduced conditions (Figure S2E). LAFS treated rec. PfP2 tetramer at three-time points, did not get resolve to a monomer however a faint band of monomer was observed due to the reduction of dimers into monomer after boiling (Figure S2E). That is why in the same urea gel, under non boiling conditions, in the lane of rec. PfP2 and at three time points of LAFS treatment, dimers were visible (Figure S2E). When LAFS from human serum was incubated with rec. PfP2 at 37°C for 3h and for varying time, rec. PfP2 transformed into a tetramer that was denaturant resistant under 4M urea (Figures S2F–S2H). All these observations strongly suggested that LAFS treatment led to the formation of a unique tetramer assembly possibly through covalent linkages amongst amino acids of four rec. PfP2 monomers.

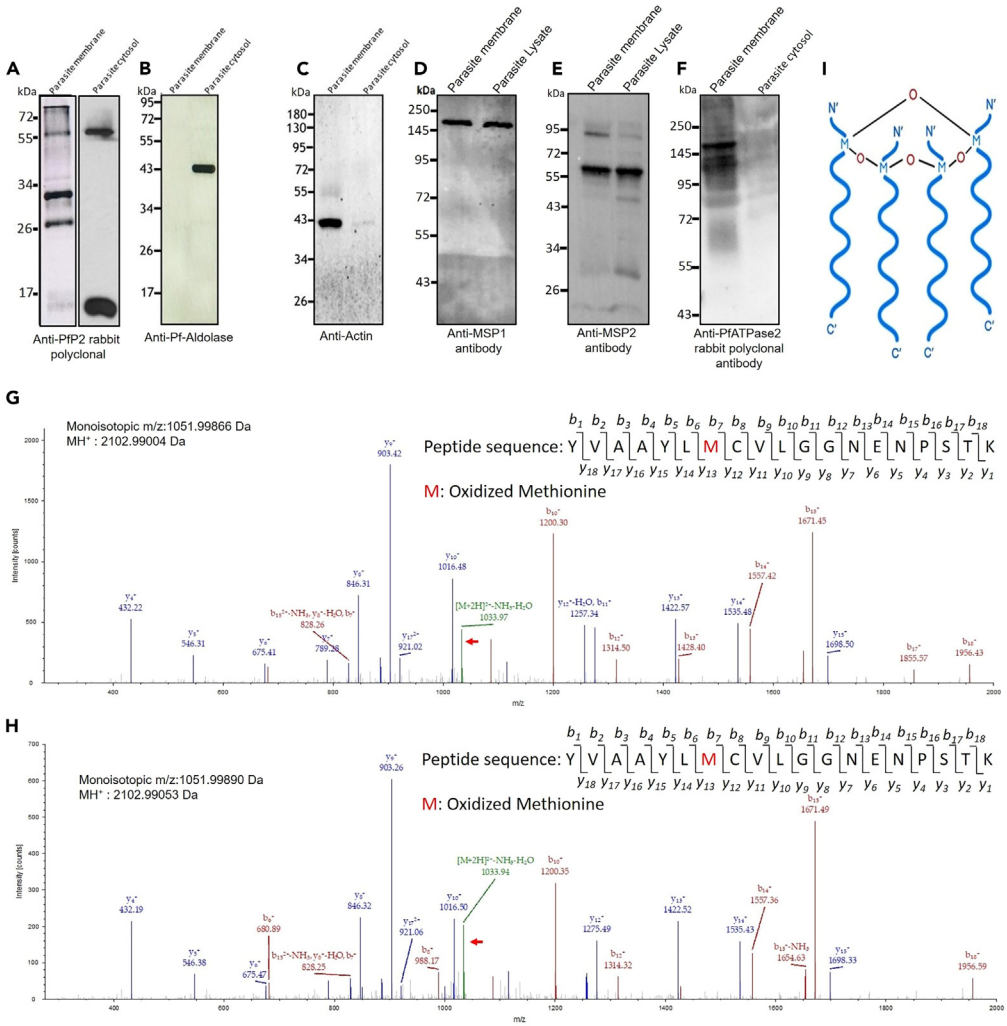

Figure 2. PfP2 oligomer localizes in the parasite plasma membrane and denaturation resistance is due to methionine oxidation and inter-peptide covalent linkage formation

(A–F) Western blot analysis of parasite membrane proteins, parasite cytosol and parasite lysate were assessed using anti-PfP2 rabbit polyclonal antibody, anti -*P. falciparum* aldolase, anti-actin, anti-MSP1, anti-MSP2, and anti-PfATPase2.

(G) ESI-MS/MS spectra of PfP2 localized in the parasite plasma membrane, the X axis depicts m/z and the Y axis shows intensity (counts). Identified P2 peptide is shown with oxidized methionine and the m/z peak has been shown with a red arrow.

(H) ESI-MS/MS spectra of the tetramer of the PfP2 peptide after LAFS treatment. The x axis depicts m/z and the Y axis shows intensity (counts). Identified P2 peptide is shown with oxidized methionine and the m/z peak has been shown with a red arrow.

(I) Model showing the possible mechanism of the formation of denaturation-resistant PfP2 tetramer with the oxidized sulfur atom in methionine residues.

PfP2 traverse through the parasite plasma membrane for its export to the IE surface. To address (1) like IE surface, whether PfP2 in the parasite plasma membrane also exists as a denaturation resistant tetramer and (2) other than PfP2 tetramer do we see any other oligomeric species, we isolated parasite plasma membrane proteins and checked for the presence of PfP2 in the preparation and its oligomeric states. We predominantly observed PfP2 dimeric and tetrameric species and a very faint monomeric band, whereas in the parasite cytosol we observed PfP2 monomers and denaturation resistant tetramer (Figures 2A and 1G). This distribution of PfP2 oligomers in the parasite plasma membrane nullify the chances of cross contamination of PfP2 from the parasite cytoplasm and also showed that monomeric PfP2 may not present in the parasite plasma membrane. Further, LAFS-induced denaturation-resistant rec. PfP2 tetramer was subjected to ESI MS/MS to detect any posttranslational modifications. Since the parasite plasma membrane showed the presence of denaturation resistant PfP2 oligomer (Figure 2A), we went ahead and did ESI MS/MS of the entire membrane preparation covered in an SDS-PAGE (from 180 kDa to 10 kDa) and searched for unique posttranslational modifications, reasons for denaturation resistance and prepared an atlas. Many proteins in the parasite membrane showed methionine oxidation (Dataset. S1). As depicted, in the parasite membrane, PfP2 exists in different oligomeric states but devoid of monomer, hence, other forms are certainly not a cytosolic contaminant as parasite aldolase and actin showed its presence

in its usual locations (Figures 2A, 2B, and 2C). Merozoite Surface Protein 1 & 2 (MSP1, MSP2) and P-type ATPase2 (PfATPase2) both showed its membrane localization confirming the cleanliness of the parasite membrane preparation (Figures 2D, 2E, and 2F). One peptide of PfP2 in the membrane preparation was identified, N′-YVAAYLMCVLGGNENPSTK-C′, where the 11th methionine residue (Met11) was oxidized (Figure 2G). Now, we went ahead to identify the same peptide in the LAFS induced denaturation resistant rec. PfP2 tetramer to check whether Met11 was also oxidized there. Surprisingly, it was (Figure 2H). In both the chromatogram of this peptide, oxidized methionine mediated PfP2 dimer peaks were denoted by a red arrow. In *Escherichia coli*, methionine oxidation in L12 (orthologue of PfP2) resulted in the detachment of L12 from the 50S ribosomal subunit.[35] Methionine oxidation in protein is involved in many biological functions where oxidation is primarily occurring due to Reactive Oxygen Species (ROS).[35,36] Intrinsically disordered proteins where exposed methionines are more prone to oxidation by ROS as opposed to mitochondrial proteome where methionines are more protected.[36] In addition to the disulfide bond, cysteine residues in albumin are susceptible to oxidation by ROS, thus important for scavenging ROS and also required for cellular signaling and communications in different cellular contexts.[36] Due to elevated ROS levels at the trophozoite stage because of hemoglobin degradation and hemozoin formation,[37–39] the S atom in the methionine residues of PfP2 possibly getting oxidized. Indicated peak and its corresponding mass (mass: 1033.97/1033.94 Dalton) of Met11 oxidized PfP2 in the parasite membrane and in LAFS treated tetramer (Figures 2G and 2H) seem to suggest the formation of ^{Met11}S-*O*-S^{Met11} linkages among four PfP2 peptide (Figure 2I) giving rise to denaturation resistant PfP2 dimer to tetramer.

PfP2 tetramer on the IE surface imports serum FAs

During IE schizogony, the malarial parasites have an enormous requirement for FAs and PL.[17,18] Salvage through import and *de novo* biosynthesis of FAs both are operational in malaria parasites depending on the type of mammalian cells that are infected and supporting the parasite's schizogony.[14,17,18] FAs and other lipid species appear to be scavenged by the parasites from the host milieu during IE development.[17,18] During the increase in volume from the ring stage to trophozoite, raw materials for PL biosynthesis for membrane fusion appear to be coming from the scavenged FAs.[17] However, during active membrane biogenesis for S/M phase and subsequent cytokinesis, parasites in addition to the scavenged FAs, appear to require an active mechanism for FAs import from human serum. During IE development, there is no *de novo* biosynthesis of FAs, hence, the requirement appears to be fulfilled through the exogenous import whereas during liver and mosquito stages, the active FAS type II pathway in the parasite apicoplast is responsible for endogenous FAs biosynthesis.[40–47] The FAS-II pathway is responsible for the elongation of FAs via the action of four distinct enzymes: FabG, FabZ, FabI, and FabB/F.[41,44,45] Interestingly, when these enzymes/genes were deleted from blood stage parasites, the effect on growth rate was minimal suggesting an active mechanism of FAs import from serum through a protein complex on the IE surface. Previously, it has been reported that at the onset of intraerythrocytic schizogony, selective removal of palmitic acid and oleic acid from the culture medium led to the downstream arrest of karyokinesis[29–32] and the imported FAs get incorporated into the parasite's triglycerides (TG).[33] The FAs import coincides with the time that PfP2 localizes on the IE surface which led us to hypothesize that insufficient FAs import due to the inhibition of PfP2 tetramer might trigger a checkpoint like response which might be abrogating growth and nuclear division of the parasites. To resolve what denaturation resistant PfP2 tetramer on the IE surface is binding to, rec. PfP2 was incubated with LAFS (albumax/human serum). LAFS was prepared (Figure 3A) and incubated with rec. PfP2. LAFS induced rec. PfP2 tetramer (Figure 3B) was subjected to nonreductive LC-MS to detect LAFS components imprisoned in rec. PfP2 tetramer. At different retention times, peaks observed in LC-MS corroborated with adduct masses of FAs and PLs. These peaks were majorly absent in LC-MS of control rec. PfP2 tetramer (Figures 3C and 3D).

To verify the LC-MS findings, the interaction between rec. PfP2 and two synthetic FAs, e.g., oleic acid and palmitic acid were assessed using isothermal titration calorimetry (ITC) (Figures 3E–3G). FAs and rec. PfP2 interactions showed binding cooperativity with gradual saturation of exothermic peak length (Figures 3E and 3F). Another ribosomal protein P1[26] as a control, did not show any interaction with oleic acid (Figure 3G), which suggested a specific interaction between oleic acid/palmitic acid and rec. PfP2. Atomic force microscopy (AFM) based elucidation of structure of native rec. PfP2 tetramer and palmitic acid bound rec. PfP2 tetramer showed a conformational switching between FA bound/unbound states (Figures 3H and 3I). However, rec. PfP2 and FAs interaction did not necessarily prove its direct import through PfP2 tetramer on the IE surface.

At the trophozoite stage, when PfP2 tetramer on the IE surface was made inaccessible to FAs by anti-PfP2 antibody (400 ng/μL) treatment, import of NBD-palmitic acid into the parasite was significantly diminished (Figures 4A and 4B) (Video S1). Conversely, pre-immune sera treated IEs showed significant import, which appeared as green puncta in the parasite cytosol while uninfected RBCs did not show any import (Figures 4A and 4B). NBD-palmitic acid is an analogue where palmitic acid is attached with a fluorophore NBD and it was used at 10μM concentration. Flow cytometry of NBD-palmitic acid incubated IEs with/without anti-PfP2 antibody treatment also showed the fact that anti-PfP2 (400 ng/μL) antibody inhibited the import of NBD-palmitic acid (Figure 4B) (Figure S5). Together, these data suggested that the import of FAs occurs through PfP2 tetramer on the IE surface. Upon rescue (antibody washout), import of NBD-palmitic acid resumed showing quantifiable incorporation within 3h (Figures 4D and 4E). When PfP2 was conditionally downregulated at the trophozoite stage, import of NBD-palmitic acid was significantly reduced (Figure 4F) (Video S2). Upon rescue (washing out GlcN), import resumed showing quantifiable incorporation by 3-4h (Figures 4F–4H). Abrogation of import of NBD-palmitic acid was further confirmed in trophozoite stage *P. falciparum* Chloroquine resistant K1 strain and Artemisinin resistant C580Y strain parasites which were treated with anti-PfP2 (400 ng/μL) antibody and quantifiably rescued upon antibody washout (Figures 4J–4M). All these data suggested that the import of FAs in *P. falciparum* and in resistant strains of parasites occurs through PfP2 tetramer on the IE surface at the onset of parasite schizogony.

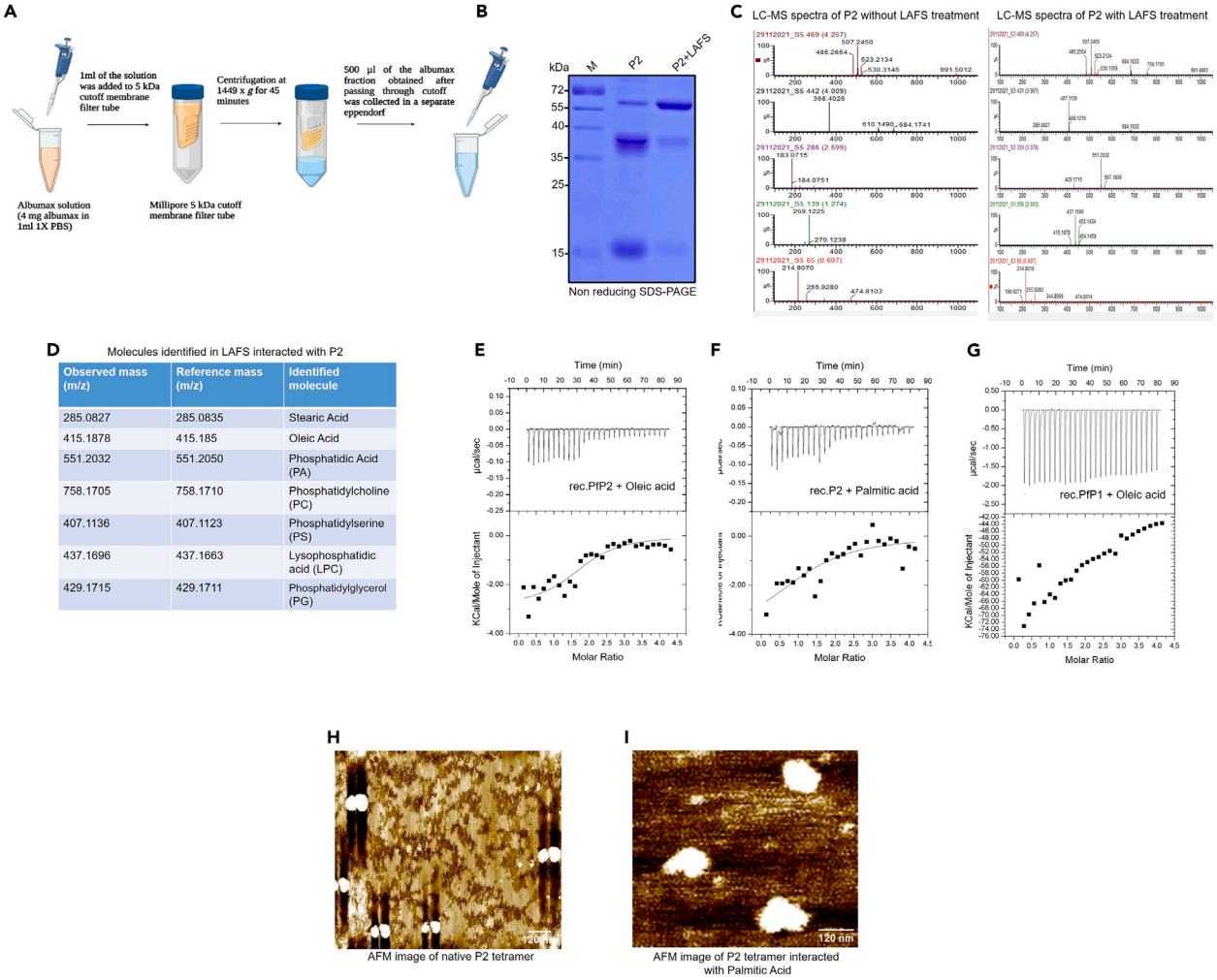

Observed mass (m/z)	Reference mass (m/z)	Identified molecule
285.0827	285.0835	Stearic Acid
415.1878	415.185	Oleic Acid
551.2032	551.2050	Phosphatidic Acid (PA)
758.1705	758.1710	Phosphatidylcholine (PC)
407.1136	407.1123	Phosphatidylserine (PS)
437.1696	437.1663	Lysophosphatidic acid (LPC)
429.1715	429.1711	Phosphatidylglycerol (PG)

Figure 3. PfP2 interacts with serum FAs and PLs

(A) Schematic showing the method of LAFS preparation.

(B) 0.7 µg of 6x His tag rec. PfP2 was treated with LAFS for 3h at 37°C and separated in non-reducing SDS-PAGE. rec. PfP2 in 1x PBS for 3h at 37°C was used as a control.

(C) LC-MS profile at different retention times of trypsin digested but not DTT and not iodoacetamide (IAA) treated tetrameric rec. PfP2 (control) shows the different masses of P2 peptides that were generated from natively folded rec. PfP2 tetramer. LC-MS profile at different retention times of LAFS treated rec. PfP2 tetramer which was trypsin digested but not DTT and iodoacetamide treated. LC-MS profile depicting different masses unrelated to control panel. In the LC-MS profile, the X axis represents m/z and the Y axis represents % abundance.

(D) List of molecules in LAFS that interacted with rec. PfP2 tetramer identified by calculating adduct masses of each molecule found in panel C. To identify molecules using their adduct mass, www.lipidmaps.org was mainly used. In addition,refs. [48–50] were also referred.

(E–G) Isothermal titration calorimetry (ITC) showing interactions between rec. PfP2 and oleic acid/palmitic acid. As a control, recombinant Plasmodium P1 protein[26] was checked for its interaction with Palmitic acid.

(H and I) Atomic force microscopy (AFM) images of native rec. PfP2 tetramer and palmitic acid bound rec. PfP2 tetramer.

$^{12/53}$Cys-Cys$^{12/53}$ redox switch in PfP2 tetramer regulates FAs binding and release

We hypothesize that denaturation resistant PfP2 tetramer in IE ghost interacts with FAs. Mechanistically in this interaction, oxidation/reduction (redox switch) of cysteine residues in PfP2 tetramer appear to be involved in the binding and release of FAs. To explore this hypothesis, rec. PfP2 was pre-reduced with DTT, then alkylated using Iodoacetamide (IAA) to prevent reformation of disulfide linkages and followed by LAFS treatment. When LAFS-induced alkylated rec. PfP2 tetramer was subjected to LC-MS to detect whether it can bind FAs, astonishingly denaturation resistance was retained but none of the peak of adduct masses matched with any FAs. This suggested the involvement of cysteine residues in rec. PfP2 tetramer for its interaction with serum FAs (Figures S3A–S3C). This indicated that Cys-Cys disulfide linkages may be important for FAs interactions in rec. PfP2 tetramer. PfP2 consists of two cysteine residues, at the 12th and 53rd positions. To understand whether both the cysteine residues or either 12th or 53rd are required for FAs interactions, we performed Site-Directed Mutagenesis

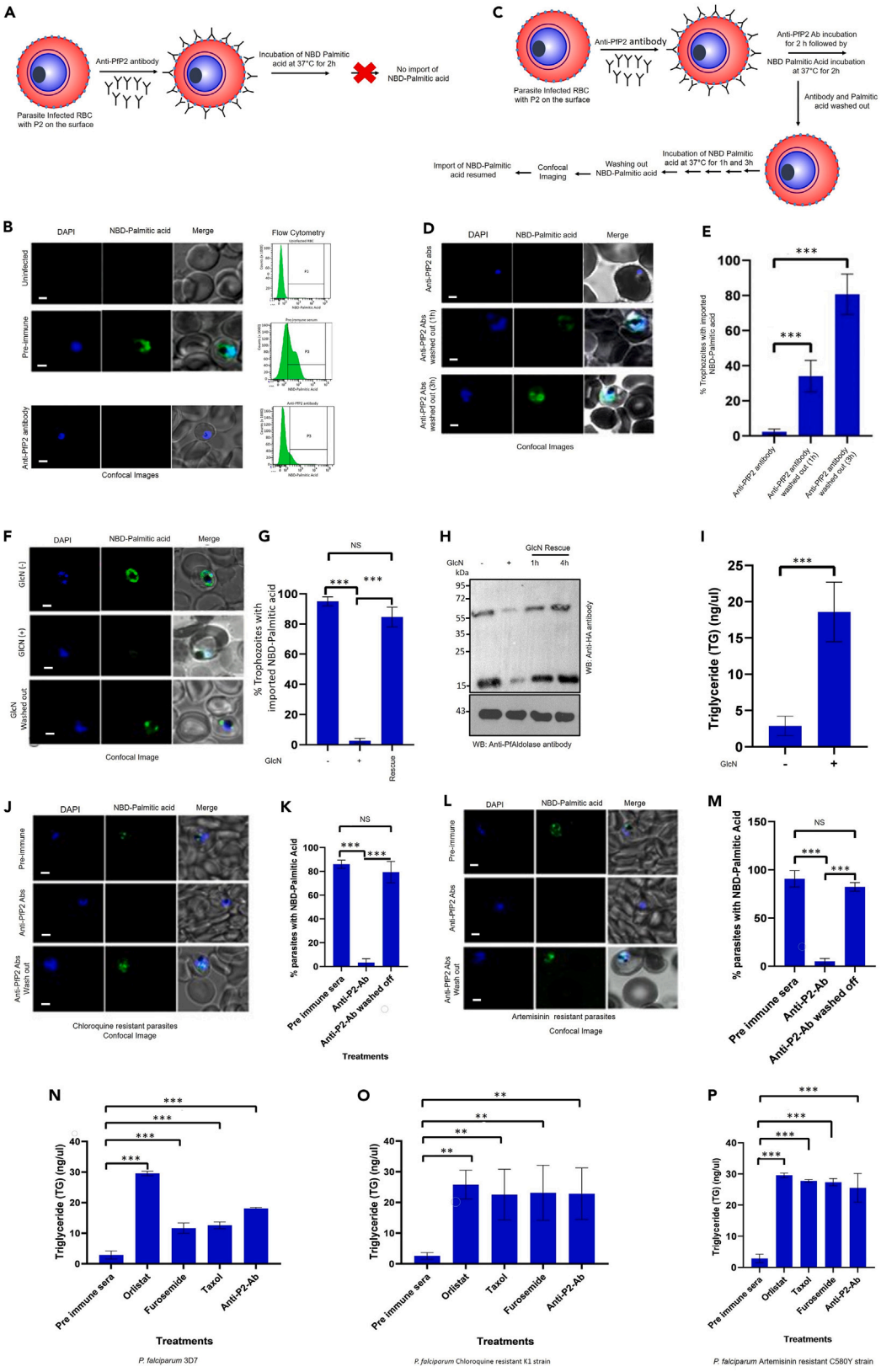
A
Anti-PfP2 antibody
Incubation of NBD Palmitic acid at 37°C for 2h
No import of NBD-Palmitic acid
Parasite Infected RBC with P2 on the surface
C
Anti-PfP2 antibody
Anti-PfP2 Ab incubation for 2 h followed by
NBD Palmitic Acid incubation at 37°C for 2h
Antibody and Palmitic acid washed out
Incubation of NBD Palmitic acid at 37°C for 1h and 3h
Washing out NBD-Palmitic acid
Confocal Imaging
Import of NBD-Palmitic acid resumed
Parasite Infected RBC with P2 on the surface
B
DAPI
NBD-Palmitic acid
Merge
Flow Cytometry
Uninfected
Pre-immune
Anti-PfP2 antibody
Confocal Images
D
Anti-PfP2 abs
Anti-PfP2 Abs washed out (1h)
Anti-PfP2 Abs washed out (3h)
Confocal Images
E
% Trophozoites with imported NBD-Palmitic acid
Anti-PfP2 antibody
Anti-PfP2 antibody washed out (1h)
Anti-PfP2 antibody washed out (3h)
F
GlcN (-)
GlCN (+)
GlcN Washed out
Confocal Image
G
% Trophozoites with imported NBD-Palmitic acid
GlcN
Rescue
H
GlcN Rescue
GlcN
kDa
WB: Anti-HA antibody
WB: Anti-PfAldolase antibody
I
Triglyceride (TG) (ng/ul)
GlcN
J
Pre-immune
Anti-PfP2 Abs
Anti-PfP2 Abs Wash out
Chloroquine resistant parasites
Confocal Image
K
% parasites with NBD-Palmitic Acid
Pre immune sera
Anti-P2-Ab
Anti-P2-Ab washed off
Treatments
L
Artemisinin resistant parasites
Confocal Image
M
% parasites with NBD-Palmitic Acid
Pre immune sera
Anti-P2-Ab
Anti-P2-Ab washed off
N
Triglyceride (TG) (ng/ul)
Pre immune sera
Orlistat
Furosemide
Taxol
Anti-P2-Ab
Treatments
P. falciparum 3D7
O
Triglyceride (TG) (ng/ul)
Pre immune sera
Orlistat
Taxol
Furosemide
Anti-P2-Ab
Treatments
P. falciparum Chloroquine resistant K1 strain
P
Triglyceride (TG) (ng/ul)
Pre immune sera
Orlistat
Taxol
Furosemide
Anti-P2-Ab
Treatments
P. falciparum Artemisinin resistant C580Y strain

Figure 4. PfP2 tetramer on the IE surface imports serum FAs

(A) Schematic showing the import of NBD-Palmitic acid in the absence/presence of anti-PfP2 antibody.

(B) Confocal images and flow cytometry of NBD-palmitic acid import in uninfected or in pre-immune sera (400 ng/μL) treated or anti-PfP2 antibody (400 ng/μL) treated infected RBCs.

(C) Schematic showing the process of the inhibition of import of NBD-palmitic acid in the presence of anti-PfP2 antibody and resume of fatty acid import after antibody wash out.

(D) Confocal images of NBD-palmitic acid import in the presence of anti-PfP2 antibody (400 ng/μL) or after 1h or 3h of anti-PfP2 antibody washout (Rescue).

(E) Quantification of % trophozoite stage parasites showing NBD-Palmitic acid import in the presence of anti-PfP2 antibody (400 ng/μL) or after 1h or 3h of anti-PfP2 antibody washout ($N = 3$).

(F) Confocal images of NBD-palmitic acid import in PfP2-HA transgenic parasites in the absence/presence of 3mM GlcN or after 4h of GlcN washout (rescue).

(G) Quantification of % trophozoite stage parasites showing NBD-palmitic acid import in the absence/presence of 3mM GlcN or after 4h of GlcN washout ($N = 3$).

(H) Western blot analysis of the expression of PfP2-HA in the absence/presence of 3mM GlcN or after 1h or 4h of GlcN washout. PfP2 was probed with anti-HA antibody and as a loading control Plasmodium aldolase antibody was used.

(I) Quantification of Triglyceride (TG, ng/μL) of PfP2-HA transgenic parasites at trophozoite stage in the absence/presence of 3mM GlcN ($N = 3$).

(J) Confocal images of NBD-palmitic acid import in chloroquine resistant K1 strain in the presence of pre-immune sera (400 ng/μL) or anti-PfP2 antibody (400 ng/μL) and after 3h of anti-PfP2 antibody washout (Rescue).

(K) Quantification of % trophozoite stage K1 parasites showing NBD-Palmitic acid import in the presence of pre-immune sera (400 ng/μL) or anti-PfP2 antibody (400 ng/μL) and after 3h of anti-PfP2 antibody washout ($N = 4$).

(L) Confocal images of NBD-palmitic acid import in Artemisinin resistant C580Y strain in the presence of pre-immune sera (400 ng/μL) or anti-PfP2 antibody (400 ng/μL) and after 3h of anti-PfP2 antibody washout (Rescue).

(M) Quantification of % trophozoite stage C580Y parasites showing NBD-palmitic acid import in the presence of pre-immune sera (400 ng/μL) or anti-PfP2 antibody (400 ng/μL) and after 3h of anti-PfP2 antibody washout ($N = 3$).

(N) Quantification of triglyceride (TG, ng/μL) at trophozoite stage of Pf3D7 parasites after the treatment with pre-immune sera (400 ng/μL), Orlistat (10μM), Furosemide (20 μM), Taxol (0.5 μM), anti-PfP2 antibody (400 ng/μL) ($N = 4$).

(O) Quantification of triglyceride (TG, ng/μL) at trophozoite stage of K1 parasites after the treatment with pre-immune sera (400 ng/μL), Orlistat (10μM), Furosemide (20 μM), Taxol (0.5 μM), anti-PfP2 antibody (400 ng/μL) ($N = 3$).

(P) Quantification of triglyceride (TG, ng/μL) at trophozoite stage of C580Y parasites after the treatment with pre-immune sera (400 ng/μL), Orlistat (10μM), Furosemide (20 μM), Taxol (0.5 μM), anti-PfP2 antibody (400 ng/μL) ($N = 3$). Scale bar 2 μm. N represents biological replicates. All quantitative experiments were repeated at least three times or more as indicated. Significance was considered at $*p < 0.05$, $**p < 0.01$, $***p < 0.001$

(SDM) and generated three clones, Clone 1 (C12A), Clone 2 (C53A), Clone 3 (C12A + C53A) where 12th, 53rd and both the cysteines were replaced by Alanine individually and together respectively (Figures 5A, 5D, and 5G). Western blots of purified proteins from these clones under nonreducing SDS-PAGE indicated that 53rd cysteine residue is important for disulfide linkages in PfP2 oligomers because C12A replacement did not abolish disulfide bond mediated dimer formation. Whereas C53A and C12A + C53A replacements did abolish higher oligomer formation (Figures 5B, 5E, and 5H). To understand further the importance of individual cysteine residue in FAs binding, ITC of C12A (Clone 1), C53A (Clone 2), and C12A + C53A (Clone 3) were performed with palmitic acid. ITC clearly showed no interaction cooperativity as opposed to wild-type rec. PfP2 (Figures 5C, 5F, 5I, 3E, and 3F). This suggested that a single cysteine replacement either at 12th or 53rd position is enough to abrogate FAs binding to PfP2 (Figures 5C, 5F, and 5I). These observations indicated that under the oxidized condition of cysteines, FAs are interacting whereas under reduced conditions, FAs do not bind. In the resistant PfP2 tetramer, overall, oxidation/reduction of 4 disulfide linkages are required to bind and subsequent release of FAs hence one C to A replacement either at the 12th or 53rd position did not allow the interaction with FAs.

In IEs, ^{11}Met-*O*-Met^{11} mediated denaturation resistant PfP2 tetramers on the IE surface import serum FAs which is necessary for membrane biogenesis during schizogony. Mechanistically, $^{12/53}$Cys-Cys$^{12/53}$ redox switch in denaturation resistant PfP2 tetramer appears to regulate FAs binding and release on the IE surface. To ascertain the mechanism of FAs release due to cysteine reduction, LAFS-treated rec. PfP2 tetramer and NBD-palmitic acid were allowed to interact, and thereafter, Cys-Cys disulfide linkages were reduced by DTT to check whether reduced denaturation resistant rec. PfP2 tetramer can still hold bound NBD-palmitic acid. The fluorescent intensity of NBD-palmitic acid in the typhoon image clearly dropped significantly when cysteines were reduced by DTT (Figure 6A). This suggested that under oxidized state, FAs interacted and get released when cysteines were reduced. Additionally, LAFS treated denaturation resistant rec. PfP2 tetramer in the absence of DTT did interact with palmitic acid whereas in the presence of DTT we did not see any interaction, which suggested the importance of oxidized/reduced state of cysteine residues for this interaction (Figure 6B). In the parasite cytosol, monomeric PfP2 and denaturation resistant PfP2 tetramer were observed[26] and it has also been seen that FAs induce rec. PfP2 tetramerization (Figure 3B; Figure S2B). Distribution of P2 species in IEs distinctly showed that the monomeric PfP2 remained confined in the parasite cytosol whereas denaturation resistant PfP2 tetramer was found to be exported out on to the IE surface and in the IE cytosol.[25,26] This suggested that tetramerization of PfP2 in the parasite cytosol might be a prerequisite condition for its trafficking to the host cell. Denaturation resistant PfP2 tetramerization in the parasite cytosol may be forming the cleft for FAs binding and might also be fulfilling the prerequisite condition for its export. Denaturation resistant PfP2 tetramer on the IE surface binds FAs and changes its conformation. So, the sequence of events in the parasite appears to be first, the formation of denaturation resistant PfP2 tetramer in the parasite cytosol, second, the trafficking of denaturation resistant PfP2 tetramer to the host cell cytosol and to the IE surface and third, binding of FAs in the cleft of PfP2 tetramer for its import into the parasites.

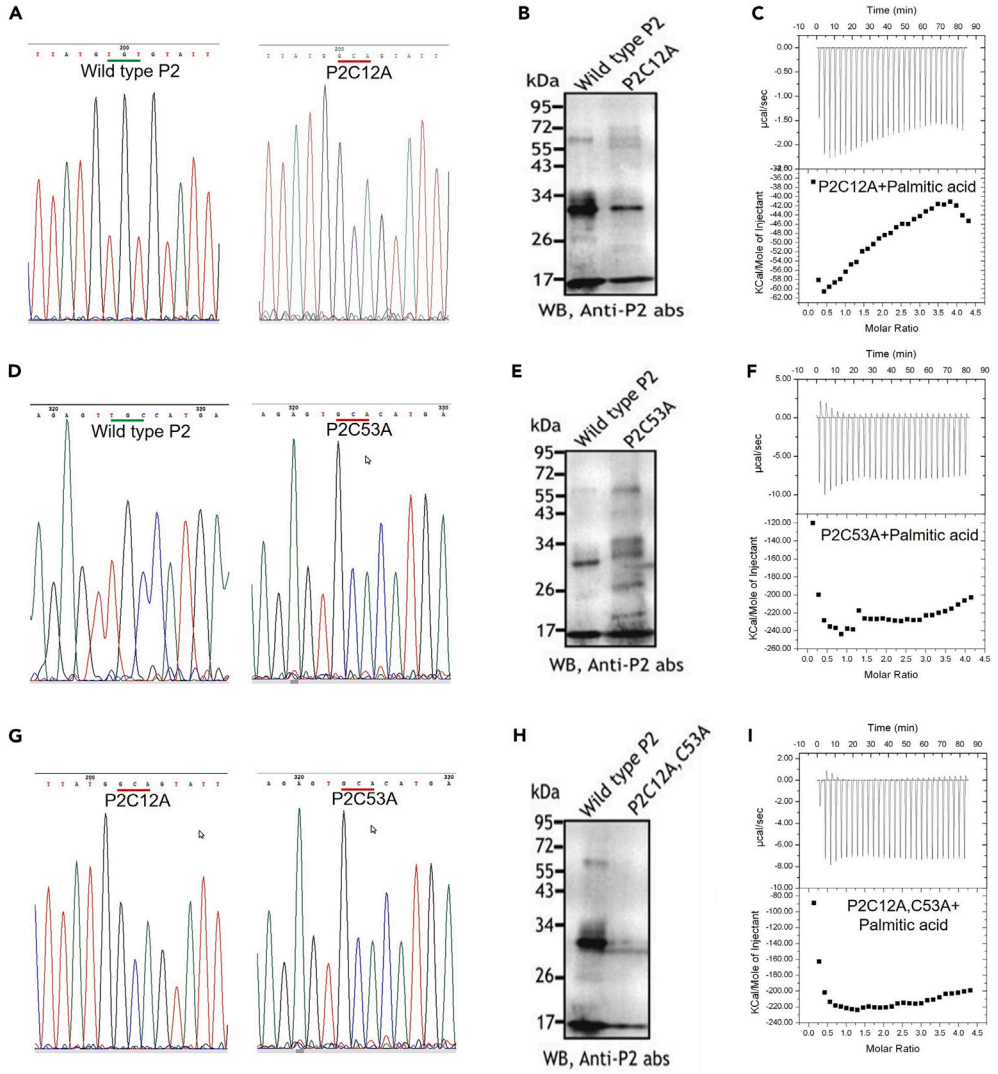

Figure 5. In PfP2 tetramer both 12th and 53rd Cysteine residues are required to bind and release FAs

(A) DNA sequence after Site-Directed Mutation (SDM) at 12th position in PfP2 replacing Cysteine with Alanine (Clone 1, C12A).

(B) Western blot analysis of wild type P2 and P2C12A in non-reducing SDS-PAGE probed with anti-PfP2 antibody.

(C) Isothermal titration calorimetry (ITC) of P2C12A and Palmitic acid.

(D) DNA sequence after SDM at 53rd position in PfP2 replacing Cysteine with Alanine (Clone 2, C53A).

(E) Western blot analysis of wild type P2 and P2C53A in nonreducing SDS-PAGE, probed with anti-PfP2 antibody.

(F) Isothermal titration calorimetry (ITC) of P2C53A and Palmitic acid.

(G) DNA sequence after SDM at 12th and 53rd positions in PfP2 replacing both Cysteine residues with Alanine (Clone3, C12A + C53A).

(H) Western blot analysis of wild type P2 and C12A + C53A in nonreducing SDS-PAGE probed with anti-PfP2 antibody.

(I) Isothermal Titration Calorimetry (ITC) of P2C12A + P2C53A and Palmitic acid.

Import of FAs through PfP2 tetramer appears to regulate parasite schizogony

Cell cycle regulation in apicomplexan parasites is poorly explored. Particularly in Plasmodium, nothing was known previously. In mammalian cells, G1/S, G2/M, and spindle assembly checkpoints (SAC) are operational throughout the cell cycle.[51,52] The G1/S checkpoint detects surplus presence of raw ingredients for daughter cell formation which is one of the critical checkpoints which any cells go through before full commitment to cell division.[53] FAs and PLs are the key components for membrane biogenesis, hence steady supply of FAs and the conversion of TG to DG and subsequently PL synthesis are critical steps for membrane biogenesis.[17] Alternatively, synthesized acyl CoA from imported FAs might interact with glycerol 3 phosphate and lysoPC for the synthesis and PC and new membranes.[54] Cell cycle arrester orlistat[17] inhibits TG catabolism to DG. Accumulation of TG is one of the hallmark signatures of delayed cell cycle progression or cell division arrest.[55,56] Cellular TG homeostasis is the only metabolic process known which is directly regulated by

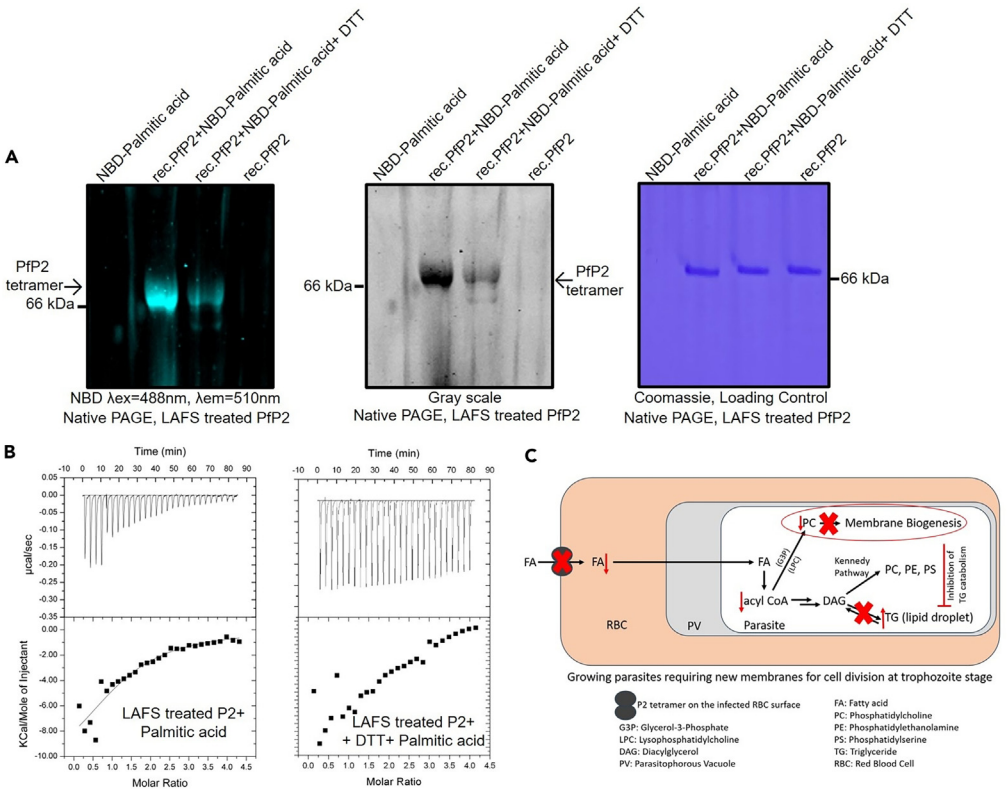

Figure 6. Involvement of $^{12/53}$Cys-Cys$^{12/53}$ redox switch for the interaction and release of FAs and overall mechanism of enhanced triglyceride (TG) as a consequence of the inhibition of FAs import through PfP2 tetramer on the IE surface

(A) Typhoon image (Color/grayscale) and Coomassie of loading control of the Native PAGE of LAFS treated rec. PfP2 incubated with NBD-Palmitic acid (P2: NBD Palmitic acid = 1:10) at 37°C for 2h followed by addition of 20 mM DTT and incubated at 37°C for another 2h. As a fluorescence control, only NBD-Palmitic acid and LAF-treated rec. PfP2 were used.

(B) Isothermal titration calorimetry (ITC) of Palmitic acid and LAFS treated denaturation resistant rec. PfP2 in the absence/presence of 20 mM DTT.

(C) Model depicting the consequence of the inhibition of FAs import through PfP2 tetramer on the IE surface at trophozoite stage.

Cdk1/Cdc28-dependent phosphorylation of key anabolic and catabolic enzymes such as Tgl4, which suggests the importance of TG and its continuous mobilization during the cell cycle progression.[55,56] It appears that there is a direct link between cell cycle regulatory kinases and TG degradation which suggests a general mechanism for coordinating membrane synthesis with cell cycle progression.[56,57] When the PfP2 tetramer on the IE surface of the parasites was blocked by anti-PfP2 antibody or when PfP2 expression was downregulated, the relative abundance of TG was significantly enhanced compared to control parasites and somewhat similar to what was observed with cell cycle inhibitor taxol or orlistat or furosemide (Figures 4I, 4N, 4O, 4P, and S4). During normal cell division process in control parasites, the membrane biogenesis pathway continues as the TG dissolute to form DG and subsequently PL[17,55–57] and or through acyl CoA mediated PC biosynthesis.[54] Hence in growing parasites at trophozoite stage, TG level was low due to its continuous dissolution. On the other hand, when FAs import was blocked using anti-PfP2 antibody or by PfP2 downregulation, TG accumulation was observed hence level of TG was elevated significantly (Figures 4I and 4N). TG was accumulated may be due to the inhibition of its catabolism, hence subsequent blockage of DG and PL formation.[17,55,56] This inhibition may be compromising the subsequent membrane biogenesis. This seems to suggest that the inhibition of FAs import through PfP2 tetramer on the IE surface overall affects the lipid availability and membrane biogenesis, which then might be creating a negative signal through a membrane sensing checkpoint.[57] This negative signal may be reversibly halted the nuclear division until the problems of FAs import and new membrane biosynthesis are fixed. Upon rescue, import of FAs resumed, and nuclear division proceeded and completed the schizogony due to the catabolism of TG to DG and PL and membrane biosynthesis (Figures 4F, 4D, S1I, and S1J). During IE development of the parasites, there is no *de novo* biosynthesis of FAs, hence the role of PfP2 tetramer on the IE surface possibly as an importing complex appeared to be important. Interestingly, PfP2 tetramer and dimer both have also been found in the parasite plasma membrane (Figure 2A), which seems to suggest that after FAs import from the IE surface, PfP2 on the parasite membrane might be playing a role to take up FAs from the infected RBC cytosol into the parasite cytosol for its final assimilation into PL biosynthesis and membrane biogenesis. Hence abrogation of PfP2 tetramer inhibited FAs import which led to the reversible arrest of the parasite schizogony.

DISCUSSION

The gene expression of PfP2 is independent of the developmentally regulated rRNAs.[24] PfP2 is a 60S stalk ribosomal protein. However, in yeast, the P2 knockout strain did not show any growth defects and *P. falciparum* stalk P0 protein which is a bona fide interactor of P2, when complemented in yeast, did not require PfP2 or yeast P2 for ribosomal activity.[58] These studies suggested that PfP2 may not be essential for ribosomal activity, but the PfP2 gene was found to be refractory to deletion during IE development.[26,59,60] This suggested that the localization and the function of PfP2 tetramer on the IE surface may be indispensable for the development from trophozoite to schizont stage. The blocking of PfP2 tetramer on the IE surface by E2G12[26] inhibited/reduced PfP2 tetramer interaction with its bona fide ligand(s) in the serum/culture medium, hence trophozoite stage parasites were arrested and did not proceed through schizogony. This observation in our previous report[26] posed a genuine question as to what is/are the serum component(s) binding to PfP2 tetramer on the IE surface.

In this report, we have shown that the import of serum FAs occurs through denaturation resistant PfP2 tetramer on the IE surface. The timing of the localization of PfP2 tetramer on the IE surface and the onset of parasite nuclear division appear to be coinciding. In *Plasmodium*, repeated DNA replication, mitosis (S/M Phase) and daughter nuclei formation precede cytoplasmic division and progeny cell formation. Inhibition of microtubule depolymerization using taxol, may not allow replicated chromosomes to segregate hence daughter nuclei formation and S/M repetition may not proceed.[10,11] At this stage, denaturation resistant PfP2 tetramer was found to be present on the IE surface, hinting at its possible role at the onset of parasite schizogony. In previous reports,[26–28,61–65] using FM4-64 and NMR, a possibility of PfP2 tetramer being involved in lipid interaction on the IE surface was indicated. It was not known about the specific class of lipid which was the bona fide ligand to the PfP2 tetramer on the IE surface.

Methionine oxidation appears to be an important posttranslational modification detected in many parasite membrane proteins (Data S1). Whether methionine oxidation has any role in protein export and in the function of membrane proteins through protein oligomerization are still under speculation and need in-depth investigation. But at least, $^{12/53}$Cys-Cys$^{12/53}$ redox switch in denaturation resistant PfP2 tetramer distinctly mediates interaction with serum FAs for its import into the parasites at the onset of IE schizogony. Inhibition of PfP2 by genetic knockdown or anti-PfP2 antibody mediated blockage resulted in the reversible arrest of nuclear division at the onset of schizogony plausibly due to the abrogation of import of serum FAs through PfP2 tetramer. As a consequence of the inhibition of import, enhanced TG concentration was observed in the parasites. As described in the model, due to reduced exogenous FAs in the parasites, the abundance of acyl CoA coming from FAs might drop and as a consequence the PC biosynthesis from acyl CoA, Glycerol-3-Phosphate and LysoPC may also be getting compromised (Figure 6C). Reduced level of PC may lead to plasma membrane malformation. This compromised membrane biogenesis may lead to the generation of arrest signal[57] and as a consequence the catabolism of TG may be getting reduced because of the low requirement of DAG. TG accumulation due to the inhibition of import of FAs and the perturbation of membrane biogenesis appear to be necessary steps to generate a negative signal which reversibly halted trophozoite growth hence did not allow parasite nuclear division and schizogony. The FAs import through PfP2 tetramer on the IE surface appears to regulate the process of schizogonic nuclear division through the relative abundance of TG and the feasibility of the downstream membrane biogenesis process. The timing of FAs import and the onset of the S/M phase seem to be overlapping. TG homeostasis is directly regulated by Cdk1/Cdc28 dependent phosphorylation of key metabolic enzymes such as Tgl4, which indicates the importance of TG and its continuous catabolism during cell division processes.[55,56] Cell-cycle-regulatory kinases and TG catabolism appear to be directly linked which suggests a general mechanism for coordinating membrane biogenesis with nuclear division and cytokinesis.[55,57]

In malarial parasites, it was previously shown that the selective removal of palmitic acid and oleic acid from the parasite culture medium resulted in the arrest of nuclear division at the onset of the S/M Phase and the imported FAs do get incorporated into the newly formed parasite plasma membrane.[29–33] After FAs import through PfP2 tetramer on the IE surface, the translocation to the parasite is elusive but speculated to be through START (Steroidogenic Acute Regulatory Protein-related Lipid Transfer) domain protein, which is known to transport phospholipids in malaria infected RBCs.[66]

There appear to be two paths to achieve a regulation at the onset of parasite schizogony, (1) through the involvement of Cyclin-CDKs and other cell division markers and (2) through the regulation of membrane biogenesis and lipid checkpoints.[67] So, in the second case, any problem in the downstream membrane biogenesis may generate a negative signal which may reversibly arrest the upstream energy and resource requiring cell biological events, such as nuclear division. However, the perturbation of membrane biogenesis may eventually require the involvement of Cyclin-CDKs to pause parasite nuclear division until the downstream problem is fixed. In Plasmodium, FAs import mediated regulation of nuclear division and membrane biogenesis appear to be the critical steps before the full commitment to the repeated S/M phase at the onset of parasite schizogony.

Limitations of the study

We were interested to find out how exogenous FAs after its import through PfP2 tetramer on the IE surface were being transported through IE cytosol and delivered into the parasite. START domain containing proteins are known to mediate transfer of PLs, ceramide, or FAs between membranes. In *P. falciparum*, out of many exported proteins, PF3D7_0104200 have been identified as a StART domain containing protein which mediates the transport of PLs.[66] We tried to express PF3D7_0104200 gene for recombinant protein expression for its interaction study with FAs. We were unable to amplify the gene in PCR hence we could not clone for its expression. This interaction study would have revealed the role of StART domain proteins in FAs transport in the IE cytoplasm. In this study we have also shown the presence of PfP2 oligomers in the parasite plasma membrane. We do not have direct evidences of FAs interactions with the PfP2 oligomers present in parasite plasma

membrane hence it is an open question whether PfP2 oligomers in the parasite membrane is also required in FAs import from the IE cytosol into the parasites.

STAR★METHODS

Detailed methods are provided in the online version of this paper and include the following:

- KEY RESOURCES TABLE
- RESOURCE AVAILABILITY
  - Lead contact
  - Materials availability
  - Data and code availability
- EXPERIMENTAL MODEL AND STUDY PARTICIPANT DETAILS
- METHOD DETAILS
  - *P. falciparum* parasite culture
  - Treatment of *P. falciparum* infected RBCs with taxol in culture
  - Immunofluorescence assay (IFA)
  - Ghost preparation of taxol arrested *P. falciparum* infected RBCs
  - Generation of rabbit polyclonal antibodies
  - Immunoprecipitation assay (IP)
  - Immunoblotting/western blotting
  - Plasmid construction for DNA electroporation
  - Parasite line, transfection method, transgenic parasite line selection and PfP2 downregulation
  - Site Directed Mutagenesis
  - Cloning expression and purification of recombinant PfP2, PfP2C12A, PfP2C53A, PfP2C12A +C53A and Plasmodium P1 protein
  - Urea SDS-PAGE
  - Treatment of rec. PfP2 with LAFS
  - LC-MS of not reduced, not Iodoacetamide (IAA) treated in-gel trypsin digested LAFS treated recombinant PfP2 tetramer
  - Parasite membrane preparation
  - Electron spray ionization (ESI) MS/MS
  - Isothermal Titration Calorimetry (ITC)
  - Atomic Force Microscopy (AFM)
  - Import of NBD-Palmitic acid
  - Flow cytometry of live infected RBCs to assess import of NBD-Palmitic acid
  - Triglyceride (TG) quantification
- QUANTIFICATION AND STATISTICAL ANALYSIS

SUPPLEMENTAL INFORMATION

Supplemental information can be found online at https://doi.org/10.1016/j.isci.2024.109760.

ACKNOWLEDGMENTS

We thank Prof. Sanjay A. Desai from NIAID, NIH for providing pL6 and pUF1-Cas9 plasmids as a gift. We are thankful to MR4 BEI resources for Plasmodium parasite strains and other reagents. We thank Calcutta National Medical College, Kolkata, India for providing O^+ human blood and human serum. We also thank Bioklone Biotech Pvt. Ltd, Chennai, India for the synthesis of custom-made antibodies. For fundings, we are thankful to Ramalingaswami Fellowship (BT/RLF/Re-entry/40/2016), Department of Biotechnology (DBT), Govt. of India, to SD; Core Research Grant (CRG/2018/000866), SERB, Department of Science and Technology (DST), Govt. of India to SD; Medical Biotechnology Research grant (BT/PR44703/BRB/10/2013/2021) Department of Biotechnology (DBT), Govt. of India, to SD and CSIR-IICB (Institutional support) to SD.

AUTHOR CONTRIBUTIONS

S.D.: Conceptualization, designing experiments, performed experiments (parasite transfection, parasite culture, biochemical and biophysical experiments), data analysis, figure preparation, manuscript writing and editing; S.D.: L.C.-M.S. data analysis; S.D. and A.M.: Isothermal titration calorimetry (ITC), ESI MS/MS data analysis; S.D. and O.M.: Site Directed Mutagenesis, ESI MS/MS data analysis; S.D. and L.D.: TG quantification.

DECLARATION OF INTERESTS

The authors declare no competing interests.

Received: August 31, 2023
Revised: April 1, 2024
Accepted: April 15, 2024
Published: April 16, 2024

REFERENCES

1. World Malaria Report (2022.
2. Read, M., Sherwin, T., Holloway, S.P., Gull, K., and Hyde, J.E. (1993). Microtubular organization visualized by immunofluorescence microscopy during erythrocytic schizogony in Plasmodium falciparum and investigation of posttranslational modifications of parasite tubulin. Parasitology *106* (Pt 3), 223–232.
3. Arnot, D.E., and Gull, K. (1998). The Plasmodium cell-cycle: facts and questions. Ann. Trop. Med. Parasitol. *92*, 361–365.
4. Gerald, N., Mahajan, B., and Kumar, S. (2011). Mitosis in the Human Malaria Parasite Plasmodium falciparum. Eukaryot. Cell *10*, 474–482.
5. Arnot, D.E., Ronander, E., and Bengtsson, D.C. (2011). The progression of the intra-erythrocytic cell cycle of Plasmodium falciparum and the role of the centriolar plaques in asynchronous mitotic division during schizogony. Int. J. Parasitol. *41*, 71–80.
6. Francia, M.E., and Striepen, B. (2014). Cell division in apicomplexan parasites. Nat. Rev. Microbiol. *12*, 125–136.
7. Doerig, C., Endicott, J., and Chakrabarti, D. (2002). Cyclin-dependent kinase homologues of Plasmodium falciparum. Int. J. Parasitol. *32*, 1575–1585.
8. Rudlaff, R.M., Kraemer, S., Streva, V.A., and Dvorin, J.D. (2019). An essential contractile ring protein controls cell division in Plasmodium falciparum. Nat. Commun. *10*, 2181.
9. Ganter, M., Goldberg, J.M., Dvorin, J.D., Paulo, J.A., King, J.G., Tripathi, A.K., Paul, A.S., Yang, J., Coppens, I., Jiang, R.H.Y., et al. (2017). Plasmodium falciparum CRK4 directs continuous rounds of DNA replication during schizogony. Nat. Microbiol. *2*, 17017.
10. Klaus, S., Binder, P., Kim, J., Machado, M., Funaya, C., Schaaf, V., Klaschka, D., Kudulyte, A., Cyrklaff, M., Laketa, V., et al. (2022). Asynchronous nuclear cycles in multinucleated *Plasmodium falciparum* facilitate rapid proliferation. Sci. Adv. *8*, eabj5362.
11. Matthews, H., Duffy, C.W., and Merrick, C.J. (2018). Checks and balances? DNA replication and the cell cycle in Plasmodium. Parasites Vectors *11*, 216.
12. Dietrich, F.S., Voegeli, S., Brachat, S., Lerch, A., Gates, K., Steiner, S., Mohr, C., Pöhlmann, R., Luedi, P., Choi, S., et al. (2004). The Ashbya gossypii genome as a tool for mapping the ancient Saccharomyces cerevisiae genome. Science *304*, 304–307.
13. Simon, C.S., Funaya, C., Bauer, J., Voβ, Y., Machado, M., Penning, A., Klaschka, D., Cyrklaff, M., Kim, J., Ganter, M., and Guizetti, J. (2021). An extended DNA-free intranuclear compartment organizes centrosome microtubules in malaria parasites. Life Sci. Alliance *4*, e202101199.
14. Botté, C.Y., Yamaryo-Botté, Y., Rupasinghe, T.W.T., Mullin, K.A., MacRae, J.I., Spurck, T.P., Kalanon, M., Shears, M.J., Coppel, R.L., Crellin, P.K., et al. (2013). Atypical lipid composition in the purified relict plastid (apicoplast) of malaria parasites. Proc. Natl. Acad. Sci. USA *110*, 7506–7511.
15. Foster, D.A., Yellen, P., Xu, L., and Saqcena, M. (2010). Regulation of G1 Cell Cycle Progression: Distinguishing the Restriction Point from a Nutrient-Sensing Cell Growth Checkpoint(s). Genes Cancer *1*, 1124–1131.
16. Stanojcic, S., Kuk, N., Ullah, I., Sterkers, Y., and Merrick, C.J. (2017). Single-molecule analysis reveals that DNA replication dynamics vary across the course of schizogony in the malaria parasite Plasmodium falciparum. Sci. Rep. *7*, 4003.
17. Gulati, S., Ekland, E.H., Ruggles, K.V., Chan, R.B., Jayabalasingham, B., Zhou, B., Mantel, P.Y., Lee, M.C.S., Spottiswoode, N., Coburn-Flynn, O., et al. (2015). Profiling the Essential Nature of Lipid Metabolism in Asexual Blood and Gametocyte Stages of Plasmodium falciparum. Cell Host Microbe *18*, 371–381.
18. Brancucci, N.M.B., Gerdt, J.P., Wang, C., De Niz, M., Philip, N., Adapa, S.R., Zhang, M., Hitz, E., Niederwieser, I., Boltryk, S.D., et al. (2017). Lysophosphatidylcholine Regulates Sexual Stage Differentiation in the Human Malaria Parasite Plasmodium falciparum. Cell *171*, 1532–1544.e15.
19. Pessi, G., Choi, J.Y., Reynolds, J.M., Voelker, D.R., and Mamoun, C.B. (2005). In vivo evidence for the specificity of Plasmodium falciparum phosphoethanolamine methyltransferase and its coupling to the Kennedy pathway. J. Biol. Chem. *280*, 12461–12466.
20. Shunmugam, S., Arnold, C.S., Dass, S., Katris, N.J., and Botté, C.Y. (2022). The flexibility of Apicomplexa parasites in lipid metabolism. PLoS Pathog. *18*, e1010313.
21. Parreira de Aquino, G., Mendes Gomes, M.A., Köpke Salinas, R., and Laranjeira-Silva, M.F. (2021). Lipid and fatty acid metabolism in trypanosomatids. Microb. Cell *8*, 262–275.
22. Schwenk, R.W., Holloway, G.P., Luiken, J.J.F.P., Bonen, A., and Glatz, J.F.C. (2010). Fatty acid transport across the cell membrane: regulation by fatty acid transporters. Prostaglandins Leukot. Essent. Fatty Acids *82*, 149–154.
23. Krishnegowda, G., and Gowda, D.C. (2003). Intraerythrocytic Plasmodium falciparum incorporates extraneous fatty acids to its lipids without any structural modification. Mol. Biochem. Parasitol. *132*, 55–58.
24. Fidock, D.A., Nguyen, T.V., Dodemont, H.J., Eling, W.M., and James, A.A. (1998). Plasmodium falciparum: ribosomal P2 protein gene expression is independent of the developmentally regulated rRNAs. Exp. Parasitol. *89*, 125–128.
25. Anaguano, D., Carrie, F.B., David, W.C., and Muralidharan, V. (2022). Rapid, time-resolved proximity labeling by sbp1 identifies a porin domain protein at the malaria parasite periphery. Preprint at bioRxiv. https://doi.org/10.1101/2022.06.30.498261.
26. Das, S., Basu, H., Korde, R., Tewari, R., and Sharma, S. (2012). Arrest of nuclear division in Plasmodium through blockage of erythrocyte surface exposed ribosomal protein P2. PLoS Pathog. *8*, e1002858.
27. Das, S., Roy, B., and Chakrabarty, S. (2021). Non-ribosomal insights into ribosomal P2 protein in Plasmodium falciparum-infected erythrocytes. Microbiologyopen *10*, e1188.
28. Das, S., Sudarsan, R., Sivakami, S., and Sharma, S. (2012). Erythrocytic stage-dependent regulation of oligomerization of Plasmodium ribosomal protein P2. J. Biol. Chem. *287*, 41499–41513.
29. Mitamura, T., Hanada, K., Ko-Mitamura, E.P., Nishijima, M., and Horii, T. (2000). Serum factors governing intraerythrocytic development and cell cycle progression of Plasmodium falciparum. Parasitol. Int. *49*, 219–229.
30. Mi-Ichi, F., Kita, K., and Mitamura, T. (2006). Intraerythrocytic Plasmodium falciparum utilize a broad range of serum-derived fatty acids with limited modification for their growth. Parasitology *133*, 399–410.
31. Mi-Ichi, F., Kano, S., and Mitamura, T. (2007). Oleic acid is indispensable for intraerythrocytic proliferation of Plasmodium falciparum. Parasitology *134*, 1671–1677.
32. Asahi, H., Kanazawa, T., Hirayama, N., and Kajihara, Y. (2005). Investigating serum factors promoting erythrocytic growth of Plasmodium falciparum. Exp. Parasitol. *109*, 7–15.
33. Palacpac, N.M.Q., Hiramine, Y., Mi-ichi, F., Torii, M., Kita, K., Hiramatsu, R., Horii, T., and Mitamura, T. (2004). Developmental-stage-specific triacylglycerol biosynthesis, degradation and trafficking as lipid bodies in Plasmodium falciparum-infected erythrocytes. J. Cell Sci. *117*, 1469–1480.
34. Pouvelle, B., Farley, P.J., Long, C.A., and Taraschi, T.F. (1994). Taxol arrests the development of blood-stage Plasmodium falciparum in vitro and Plasmodium chabaudi adami in malaria-infected mice. J. Clin. Invest. *94*, 413–417.
35. Caldwell, P., Luk, D.C., Weissbach, H., and Brot, N. (1978). Oxidation of the methionine residues of Escherichia coli ribosomal protein L12 decreases the protein's biological activity. Proc. Natl. Acad. Sci. USA *75*, 5349–5352.
36. Walker, E.J., Bettinger, J.Q., Welle, K.A., Hryhorenko, J.R., and Ghaemmaghami, S. (2019). Global analysis of methionine oxidation provides a census of folding stabilities for the human proteome. Proc. Natl. Acad. Sci. USA *116*, 6081–6090.
37. Becker, K., Tilley, L., Vennerstrom, J.L., Roberts, D., Rogerson, S., and Ginsburg, H. (2004). Oxidative stress in malaria parasite-infected erythrocytes: host-parasite interactions. Int. J. Parasitol. *34*, 163–189.
38. Hunt, N.H., and Stocker, R. (1990). Oxidative stress and the redox status of malaria-infected erythrocytes. Blood Cell *16*, 499–530.
39. Ginsburg, H., and Atamna, H. (1994). The redox status of malaria-infected erythrocytes: an overview with an emphasis on unresolved problems. Parasite *1*, 5–13.

40. Jayabalasingham, B., Menard, R., and Fidock, D.A. (2010). Recent insights into fatty acid acquisition and metabolism in malarial parasites. F1000 Biol. Rep. *2*, 24.
41. Mazumdar, J., and Striepen, B. (2007). Make it or take it: fatty acid metabolism of apicomplexan parasites. Eukaryot. Cell *6*, 1727–1735.
42. Cobbold, S.A., Vaughan, A.M., Lewis, I.A., Painter, H.J., Camargo, N., Perlman, D.H., Fishbaugher, M., Healer, J., Cowman, A.F., Kappe, S.H.I., and Llinás, M. (2013). Kinetic flux profiling elucidates two independent acetyl-CoA biosynthetic pathways in Plasmodium falciparum. J. Biol. Chem. *288*, 36338–36350.
43. Schaffer, J.E. (2002). Fatty acid transport: the roads taken. Am. J. Physiol. Endocrinol. Metab. *282*, E239–E246.
44. Yu, M., Kumar, T.R.S., Nkrumah, L.J., Coppi, A., Retzlaff, S., Li, C.D., Kelly, B.J., Moura, P.A., Lakshmanan, V., Freundlich, J.S., et al. (2008). The fatty acid biosynthesis enzyme FabI plays a key role in the development of liver-stage malarial parasites. Cell Host Microbe *4*, 567–578.
45. Vaughan, A.M., O'Neill, M.T., Tarun, A.S., Camargo, N., Phuong, T.M., Aly, A.S.I., Cowman, A.F., and Kappe, S.H.I. (2009). Type II fatty acid synthesis is essential only for malaria parasite late liver stage development. Cell Microbiol. *11*, 506–520.
46. Pei, Y., Tarun, A.S., Vaughan, A.M., Herman, R.W., Soliman, J.M.B., Erickson-Wayman, A., and Kappe, S.H.I. (2010). Plasmodium pyruvate dehydrogenase activity is only essential for the parasite's progression from liver infection to blood infection. Mol. Microbiol. *75*, 957–971.
47. Ralph, S.A., van Dooren, G.G., Waller, R.F., Crawford, M.J., Fraunholz, M.J., Foth, B.J., Tonkin, C.J., Roos, D.S., and McFadden, G.I. (2004). Tropical infectious diseases: metabolic maps and functions of the Plasmodium falciparum apicoplast. Nat. Rev. Microbiol. *2*, 203–216.
48. Pellegrino, R.M., Di Veroli, A., Valeri, A., Goracci, L., and Cruciani, G. (2014). LC/MS lipid profiling from human serum: a new method for global lipid extraction. Anal. Bioanal. Chem. *406*, 7937–7948.
49. Debierre-Grockiego, F., Schofield, L., Azzouz, N., Schmidt, J., Santos de Macedo, C., Ferguson, M.A., and Schwarz, R.T. (2006). Fatty acids from Plasmodium falciparum down-regulate the toxic activity of malaria glycosylphosphatidylinositols. Infect. Immun. *74*, 5487–5496.
50. Walczak-Skierska, J., Złoch, M., Pauter, K., Pomastowski, P., and Buszewski, B. (2020). Lipidomic analysis of lactic acid bacteria strains by matrix-assisted laser desorption/ionization time-of-flight mass spectrometry. J. Dairy Sci. *103*, 11062–11078.
51. Barnum, K.J., and O'Connell, M.J. (2014). Cell cycle regulation by checkpoints. Methods Mol. Biol. *1170*, 29–40.
52. Magiera, M.M., Gueydon, E., and Schwob, E. (2014). DNA replication and spindle checkpoints cooperate during S phase to delay mitosis and preserve genome integrity. J. Cell Biol. *204*, 165–175.
53. Bertoli, C., Skotheim, J.M., and de Bruin, R.A.M. (2013). Control of cell cycle transcription during G1 and S phases. Nat. Rev. Mol. Cell Biol. *14*, 518–528.
54. Karki, N., Johnson, B.S., and Bates, P.D. (2019). Metabolically Distinct Pools of Phosphatidylcholine Are Involved in Trafficking of Fatty Acids out of and into the Chloroplast for Membrane Production. Plant Cell *31*, 2768–2788.
55. Kurat, C.F., Wolinski, H., Petschnigg, J., Kaluarachchi, S., Andrews, B., Natter, K., and Kohlwein, S.D. (2009). Cdk1/Cdc28-dependent activation of the major triacylglycerol lipase Tgl4 in yeast links lipolysis to cell-cycle progression. Mol. Cell *33*, 53–63.
56. Atilla-Gokcumen, G.E., Muro, E., Relat-Goberna, J., Sasse, S., Bedigian, A., Coughlin, M.L., Garcia-Manyes, S., and Eggert, U.S. (2014). Dividing cells regulate their lipid composition and localization. Cell *156*, 428–439.
57. Kono, K., Al-Zain, A., Schroeder, L., Nakanishi, M., and Ikui, A.E. (2016). Plasma membrane/cell wall perturbation activates a novel cell cycle checkpoint during G1 in Saccharomyces cerevisiae. Proc. Natl. Acad. Sci. USA *113*, 6910–6915.
58. Aruna, K., Chakraborty, T., Rao, P.N., Santos, C., Ballesta, J.P.G., and Sharma, S. (2005). Functional complementation of yeast ribosomal P0 protein with Plasmodium falciparum P0. Gene *357*, 9–17. https://doi.org/10.1016/j.gene.2005.04.007.
59. Bushell, E., Gomes, A.R., Sanderson, T., Anar, B., Girling, G., Herd, C., Metcalf, T., Modrzynska, K., Schwach, F., Martin, R.E., et al. (2017). Functional Profiling of a Plasmodium Genome Reveals an Abundance of Essential Genes. Cell *170*, 260–272.e8.
60. Zhang, M., Wang, C., Otto, T.D., Oberstaller, J., Liao, X., Adapa, S.R., Udenze, K., Bronner, I.F., Casandra, D., Mayho, M., et al. (2018). Uncovering the essential genes of the human malaria parasite *Plasmodium falciparum* by saturation mutagenesis. Science *360*, eaap7847.
61. Mishra, P., Choudhary, S., Mukherjee, S., Sengupta, D., Sharma, S., and Hosur, R.V. (2015). Molten globule nature of *Plasmodium falciparum* P2 homo-tetramer. Biochem. Biophys. Rep. *1*, 97–107.
62. Mishra, P., Sharma, S., and Hosur, R.V. (2014). Residue level description of in vivo self-association of Plasmodium falciparum P2. J. Biomol. Struct. Dyn. *32*, 602–612.
63. Mishra, P., Das, S., Panicker, L., Hosur, M.V., Sharma, S., and Hosur, R.V. (2012). NMR insights into folding and self-association of Plasmodium falciparum P2. PLoS One *7*, e36279.
64. Mishra, P., Dmello, C., Sengupta, D., Chandrabhan Singh, S., Kirkise, N., Hosur, R.V., and Sharma, S. (2020). Molecular study of binding of Plasmodium ribosomal protein P2 to erythrocytes. Biochimie *176*, 181–191.
65. Mishra, P., Rajagopal, S., Sharma, S., and Hosur, R.V. (2014). The C-terminal domain of eukaryotic acidic ribosomal P2 proteins is intrinsically disordered with conserved structural propensities. Protein Pept. Lett. *22* (3), 212–218.
66. van Ooij, C., Withers-Martinez, C., Ringel, A., Cockcroft, S., Haldar, K., and Blackman, M.J. (2013). Identification of a Plasmodium falciparum phospholipid transfer protein. J. Biol. Chem. *288*, 31971–31983.
67. Patel, D., Salloum, D., Saqcena, M., Chatterjee, A., Mroz, V., Ohh, M., and Foster, D.A. (2017). A Late G1 Lipid Checkpoint That Is Dysregulated in Clear Cell Renal Carcinoma Cells. J. Biol. Chem. *292*, 936–944.
68. Prommana, P., Uthaipibull, C., Wongsombat, C., Kamchonwongpaisan, S., Yuthavong, Y., Knuepfer, E., Holder, A.A., and Shaw, P.J. (2013). Inducible knockdown of Plasmodium gene expression using the glmS ribozyme. PLoS One *8*, e73783.
69. Lyko, B., Hammershaimb, E.A., Nguitragool, W., Wellems, T.E., and Desai, S.A. (2012). A high-throughput method to detect Plasmodium falciparum clones in limiting dilution microplates. Malar. J. *11*, 124.
70. Ito, D., Schureck, M.A., and Desai, S.A. (2017). An essential dual-function complex mediates erythrocyte invasion and channel-mediated nutrient uptake in malaria parasites. Elife *6*, e23485.

STAR★METHODS

KEY RESOURCES TABLE

REAGENT or RESOURCE	SOURCE	IDENTIFIER
Chemicals, peptides, and recombinant proteins		
Saponin	Sigma- Aldrich	Cat # S7900
Protease Inhibitor Cocktail	Sigma- Aldrich	Cat # P8465
BCA Reagent	TaKaRa	Cat # T9300A
Protein G-Sepharose Beads	Sigma- Aldrich	Cat # P3296
PVDF Membrane	Millipore	Cat # IPVH00010
WR99210	Sigma- Aldrich	Cat # SML2976
5-Fluorocytosine	Sigma- Aldrich	Cat # F7129
DSM1	Sigma- Aldrich	Cat # 5333040001
Glucosamine (GlcN)	Sigma- Aldrich	Cat # G1514
Phusion Site-Directed Mutagenesis Kit	Thermo Scientific	Cat # F-541
Kanamycin	Sigma- Aldrich	Cat # K1377
Ampicillin	Sigma- Aldrich	Cat # A9518
Hi-bind Ni-NTA agarose beads	Invitrogen	Cat # R901-15
Hi-bind Ni-NTA agarose beads	Roche	Cat # 05893682001
Urea	Sigma- Aldrich	Cat # U5378
Albumax II	Gibco	Cat # 11021-037
RPMI 1640	Gibco	Cat # 31-800-022
Amicon Ultra Membrane Filter cutoff	Millipore	Cat # UFC900324
Acetonitrile (ACN)	J.T Baker	Cat # MFCD00001878
Trifluoroacetic Acid (TFA)	J.T Baker	Cat # MFCD00004169
DTT	Sigma- Aldrich	Cat # 43819
Iodoacetamide	Sigma- Aldrich	Cat # I6125
Paraformaldehyde	Sigma- Aldrich	Cat # 158127
Glutaraldehyde	Sigma- Aldrich	Cat # G6257
Ammonium Bicarbonate	Sigma- Aldrich	Cat # 09830
Trypsin	Millipore	Cat # 650279
C18 Resin column	Agilent	Cat # 5188-2750
Sodium Carbonate (Na_2CO_3)	Combi-Blocks	Cat # QF-3224
Sodium Bicarbonate ($NaHCO_3$)	Combi-Blocks	Cat # QF-3795
Palmitic Acid	Sigma- Aldrich	Cat # P0500
Palmitic Acid	Combi-Blocks	Cat # QF-5127
Oleic Acid	Sigma- Aldrich	Cat # O1008
Oleic Acid	Combi-Blocks	Cat # QA-7825
NBD-Palmitic acid	Avanti Polar	Cat# 810105P
DAPI	Sigma- Aldrich	Cat # MBD0015
Hoechst 33342	Sigma- Aldrich	Cat # 14533
Concanavalin A	Sigma- Aldrich	Cat # C0412
Furosemide	Combi-Blocks	Cat # OR-4262
Taxol	Sigma- Aldrich	Cat # T7191
Orlistat	Sigma- Aldrich	Cat # O4139
Triglyceride(TG) quantification Kit	Sigma- Aldrich	Cat # MAK266

(*Continued on next page*)

Continued

REAGENT or RESOURCE	SOURCE	IDENTIFIER
Muscovite Mica Sheets	Avantor	Cat# 71856-04
ECL Reagent	TaKaRa	Cat# T7101A
EcoRI	New England Biolabs	Cat # R0101
XhoI	New England Biolabs	Cat # R0146
DpnI	New England Biolabs	Cat # R0176
BtgZI	New England Biolabs	Cat # R0703
Taq DNA Polymerase	New England Biolabs	Cat # M0273
Q5 Hi Fidelity DNA Polymerase	New England Biolabs	Cat # M0491
Phusion Hi Fidelity DNA Polymerase	New England Biolabs	Cat # M0530
Phusion Site-Directed Mutagenesis Kit	Thermo Scientific	Cat # F-541
T4 DNA Ligase	New England Biolabs	Cat # M0202
Oligonucleotides (Table S1)	Integrated DNA Technologies	https://www.idtdna.com/
Antibodies		
Anti-PfP2 Rabbit polyclonal	Bioklone Biotech Pvt. Ltd (www.bioklone.com)	This study
Anti-PfP2 Mabs, E2G12	Bioklone Biotech Pvt. Ltd (www.bioklone.com)	Das et al.[26]
Anti-PfATPase2 Rabbit Polyclonal	Bioklone Biotech Pvt. Ltd (www.bioklone.com)	This study
Anti-Plasmodium Aldolase Antibody	Abcam	Cat # ab38905; RRID:AB_771788
Anti-Actin Antibody	Santacruz	Cat # SC-8432; RRID:AB_626630
Anti-β Tubulin Antibody	Sigma- Aldrich	Cat # T8328; RRID:AB_1844090
Anti-HA Antibody	Abcam	Cat # ab137838; RRID:AB_2810986
Anti-MSP1 Antibody	MR4, BEI	Cat # MRA-880A
Anti-MSP2 Antibody	MR4, BEI	Cat # MRA-834
Anti-Mouse HRP	Millipore, Sigma	Cat # 12349; RRID:AB_390192
Anti-Rabbit HRP	Millipore, Sigma	Cat # 12348; RRID:AB_390191
Anti-Mouse Alexa 488	Abcam	Cat # ab150113; RRID:AB_2576208
Anti-Rabbit Alexa 488	Abcam	Cat # ab150077; RRID:AB_2630356
Anti-Mouse Alexa 647	Abcam	Cat # ab150115; RRID:AB_2687948
Anti-Rabbit Alexa 647	Abcam	Cat # ab150083; RRID:AB_2714032
Bacterial and virus strains		
P. falciparum 3D7 Strain	MR4, BEI	Cat # MRA-102
P. falciparum K1 Strain	MR4, BEI	MRA-159
P.falciparum CamWT_C580Y Starin	MR4, BEI	MRA-1251
P. falciparum 3D7 P2-HA glmS strain	This Lab	This Paper
Software and algorithms		
ImageJ	National Institute of Health	N.A
MicroCal ITC data processing software	MicroCal	N.A
FLOWJO	BD Biosciences	N.A
Adobe Photoshop CS6	Adobe	N.A
GraphPad Prism 5	Graphpad.com	N.A
LIPID MAPS	www.lipidmaps.org	N.A
XCALIBUR	Thermo Scientific	N.A
PROTEOM DISCOVER	Thermo Scientific	N.A
PicoView 1-20.2	AFM (Agilent)	N.A
Plasmodium Database	Plasmodb.org	N.A
MassLynx V4.1	Waters	N.A

RESOURCE AVAILABILITY

Lead contact

Further information and requests for resources and reagents should be directed to and will be fulfilled by the lead contact, Sudipta Das (sudipta.das@iicb.res.in).

Materials availability

This study did generate Anti-PfP2, Anti-PfATPase2 rabbit polyclonal antibody. It has also generated PfP2-HA transgenic parasites and three site directed mutagenesis clones of PfP2.

Data and code availability

- Any additional information required to reanalyze the data reported in this paper is available from the lead contact upon request.
- This paper does not report original code.
- All relevant data are available in the manuscript and the supplemental information.

EXPERIMENTAL MODEL AND STUDY PARTICIPANT DETAILS

Plasmodium falciparum 3D7 strain, *Plasmodium falciparum* Chloroquine resistant K1 strain and *Plasmodium falciparum* Artemisinin resistant CamWT_C580Y strains.

METHOD DETAILS

P. falciparum parasite culture

P. falciparum 3D7, Chloroquine resistant K1 strain (MRA-159) and Artemisinin resistant strains, CamWT_C580Y (MRA-1251) parasites were cultured using type O^+ human RBCs in RPMI1640 supplemented with 15 mM HEPES, 2 g/L sodium bicarbonate, 10 mg/L hypoxanthine, 50 mg/L Gentamicin sulfate, and 0.5% Albumax (cRPMI). Asexual stages of *P. falciparum* were maintained at 5% hematocrit in cRPMI at 37°C in a humidified incubator containing 89% N2, 5% O2 and 6% CO2. Parasite cultures were periodically tested by PCR for *Mycoplasma* contamination to ensure that they are free from *Mycoplasma*. Parasites were synchronized using 500 mM Alanine and 10 mM HEPES, pH = 7.4. Two rounds of synchronized 6–7% ring stage parasites were used for transfections.

Treatment of *P. falciparum* infected RBCs with taxol in culture

Paclitaxel was dissolved in DMSO to make a 10x concentration. The required volume from the stock was added into the culture medium to achieve a 500 nM final concentration. *P. falciparum* parasites were synchronized two rounds using 500 mM Alanine and 10mM HEPES, pH = 7.4. After 2 generations, synchronized ring stage parasites at around 18-22h PMI were subjected to taxol treatment. After 6h of treatment, at the trophozoite stage, at around 26-30h PMI, taxol-arrested IEs were collected and washed twice with 1x PBS and used for biochemical experiments and confocal imaging.

Immunofluorescence assay (IFA)

IFA of taxol arrested IEs was performed in solution. Infected RBCs were centrifuged at 500*g* for 7 min, washed twice with 1xPBS, and resuspended in 1xPBS. Infected RBCs were fixed using 4% paraformaldehyde and 0.0075% glutaraldehyde in 1xPBS for 20 min at 4°C. All subsequent steps were carried out at room temperature (24°C–26°C). Infected RBCs were permeabilized using 0.1% Triton X-100 in 1xPBS for 30 min and washed three times with 1xPBS. 3% BSA in 1xPBS was used for blocking. Anti-HA antibody to PfP2-HA was used at 1:500 dilution in 1xPBS containing 0.01% Triton X-100 and incubated for 3–4h at room temperature. Infected RBCs were pelleted at 500x *g*, washed 3 times with 1xPBS containing 0.01% Triton X-100, and treated with appropriate Alexa 488 conjugated secondary antibodies (Molecular Probes) at 1:500 dilution for 2h at room temperature. After washing 3–4 times with 1xPBS containing 0.01% Triton X-100, IEs were incubated for 5 min with DAPI (0.1 μg/mL). IEs were imaged using a Leica confocal microscope. Model: Leica TCS SP8, Objective: 100×/60X, NA:1.4, PMT detector. Acquired IFA images were processed using ImageJ software.

Ghost preparation of taxol arrested *P. falciparum* infected RBCs

IE ghost was prepared as described in Das et al., 2012.[26] Briefly, taxol arrested IEs at about 6–7% parasitemia was pelleted at 500x *g* for 5 min and washed with cRPMI once. IE pellet was resuspended in 0.1% Saponin and protease inhibitor cocktail and 1 mM PMSF in 1xPBS, pH 7.4 for15 min at 37°C. The sample was then centrifuged for 10 min at 10,000x *g* at 4°C to get the parasite pellet and it was stored at −80°C. About 65–75% of the opaque supernatant (ghost and cytosol fraction) was gently separated to avoid cross contamination due to parasite pellet. This supernatant fraction was pelleted at 20,000x *g* for 2h at 4°C, washed twice with 1xPBS, pH 7.4, and stored at −80°C as IE ghost. After ghost precipitation, the supernatant (IE cytosol) was stored at −80°C for subsequent analysis.

Generation of rabbit polyclonal antibodies

Rabbit polyclonal antibody against recombinant PfP2 and recombinant P type ATPase2 (PfATPase2) were custom generated by Bioklone Biotech India Pvt. Company, based in Chennai, India. The monoclonal anti-PfP2 antibody E2G12[26] was also developed by the same company.

Immunoprecipitation assay (IP)

IP was performed as mentioned in Das et al., 2012.[26] Briefly, *P. falciparum* parasite pellets were suspended in 200 μL non-denaturing lysis buffer (20 mM Tris HCl pH 8.0, 137 mM NaCl, 10% glycerol, 1% NP-40, 2 mM EDTA) in the presence of protease inhibitor cocktail in ice for 15 min. Cells were briefly sonicated (Labman Scientific Instruments, Model no. Pro650) for 1 min, and centrifuged at 15,000 xg at 4°C. The supernatant was collected, the protein was estimated using BCA, and 100 μg protein was incubated with 20 μL packed protein G-Sepharose beads at 4°C for 1 h for pre-clearing. Packed Protein G Sepharose beads (20 μL) were washed repeatedly and the protein content of the pre-cleared lysate was estimated. For 3–4 μg protein lysate, 6–8 μg of anti-P2 antibody or control pre-immune serum was added. The protein-antibody solutions were incubated at 4°C for 6h on a rotary shaker, followed by incubation with 20 μL of packed Protein G-sepharose beads at 4°C for 2 h. Subsequently, the beads were centrifuged at 500 g and washed 6 times with lysis buffer. To the beads, SDS-PAGE loading buffer was added and boiled for 5 min followed by centrifugation at 15,000 x*g* for 15 min at room temperature. The supernatant was loaded on SDS-PAGE for immunoblotting.

Immunoblotting/western blotting

Recombinant PfP2 protein under non-reduced and reduced conditions were run in SDS-PAGE. On the other hand, saponin-freed parasite pellets were lysed in RIPA buffer (20 mM Tris HCl (pH 7.5), 150 mM NaCl, 1 mM Na2 EDTA, 1 mM EGTA, 1% NP-40, 1% Na-deoxycholate, 2.5 mM Na-pyrophosphate, 1 mM β-glycerophosphate) containing protease inhibitors by a brief sonication at 4°C or parasite pellet was directly lysed in SDS containing loading buffer in some experiments. The lysates were centrifuged at 15,000 xg at 4°C for 30 min and the supernatant was used for the immunoblots. Before loading, the protein was mixed with gel loading buffer (50 mM Tris HCl pH 6.8, 10 mM DTT/100 mM β-ME, 2% SDS, 0.1% bromophenol blue, 10% glycerol) and heated at 90°C for 10 min. Samples were resolved on 12% SDS–PAGE and proteins were transferred to methanol-activated polyvinylidene fluoride (PVDF) membrane using anode buffer (25 mM Tris pH 10.4, glycine, 10% Methanol) and wet transferred for 2h at 4°C. PVDF membrane was blocked with 5% skimmed milk or 5% BSA in 1x PBS overnight and probed using specific antibodies. Primary antibody dilution was made in 1x PBS containing Tween 20 (0.2%) and incubated with the membrane for 3 h at room temperature on a rocker. Primary antibody binding was detected by appropriate secondary antibodies conjugated to horseradish peroxidase (HRP). Dilution of the secondary antibody was made in 1x PBS Tween 20 (0.2%). After each incubation, the membrane was washed with 1x PBS-Tween-20 (0.2%) for 5 min at least 5–6 times. The immunoblots were developed using the chemiluminescent substrate. Anti-PfP2 antibody: 1:10K; Anti-PfP2 E2G12 monoclonal antibody: 1:2K; Anti-PfAldolase antibody: 1:5K; Anti-actin: 1:2K; Anti-HA: 1:5K, Anti-MSP1 (MRA-880A):1:2K, Anti-MSP2 (MR4):1:2K. (K = X1000)

Plasmid construction for DNA electroporation

For conditional knockdown of the PfP2 protein, homology region 1 (HR1) and HR2 were PCR amplified from the coding and intergenic region and the 3′UTR respectively with two sets of primers. Both the homology regions were cloned into the pL6-3HA-glms-ribozyme vector which contains human dihydrofolate reductase (hDHFR) as a selectable marker that confers resistance to WR99210. HR1 and HR2 PCR products were cloned one by one with the sequencing of DNA. A list of prospective 20 base nucleotide sequences (N20) for guide RNAs were generated using the Eukaryotic Pathogen CRISPR guide RNA (gRNA) design tool (http://grna.ctegd.uga.edu/) that targets the *P2 gene* in the chromosomal DNA segment flanked by the 5′ and 3′ HRs. gRNAs were cloned in pUF1-Cas9 vector which carries a gRNA expression cassette, Cas9 endonuclease expression cassette and a yeast dihydroorotate dehydrogenase (yDHODH) cassette for selection with DSM1. For the oligonucleotide sequences used to generate plasmid constructs were mentioned ion Table S1.

Parasite line, transfection method, transgenic parasite line selection and PfP2 downregulation

P. falciparum 3D7 parasites was used to generate transgenic parasites. Standard transfection method, parasite selection and negative selection with 5FC and limiting dilution to select integrated parasites were followed as described in Prommana et al.,[68] Lyko et al.,[69] and Ito et al.,.[70] Briefly, Pf3D7 ring-stage parasites from a culture at 6–7% parasitemia were washed three times with pre-warmed Cytomix (pH = 7.4) and then resuspended with an equal volume of ice-cold Cytomix. An aliquot of 250 μL of ring stage parasite suspension was mixed with 50 μg of both the plasmids and put in 0.2 cm cuvette for electroporation. BioRad Gene Pulser was set at 0.31 kV and 950 μF. Parasite cultures were selected using 5nM WR99210 and 1.5μM DSM1. After 2–3 weeks of transfection, parasites were detected using Giemsa staining. PCR was used to evaluate the integration of the hDHFR and glmS.

For Conditional downregulation of P2 protein under the glmS ribozyme system, 3 mM GlcN was added to synchronous ring stage parasites at around 12-14h PMI (Prommana et al.,[68]). GlcN exposure was continued for up to 10h before washout and rescue experiments or kept continued before harvest for phenotype studies by fixation and IFA and biochemical experiments. Control experiments with GlcN added in the culture media revealed no measurable toxicity in wild-type *P. falciparum* 3D7 parasites at up to a 4 mM concentration.

Site Directed Mutagenesis

Site-Directed Mutagenesis (SDM) of the PfP2 gene was done to achieve three clones, Clone 1 (C12A), Clone 2 (C53A) and Clone 3 (C12A C53A). Briefly, three mutated constructs were created using SDM, which entails creating primers that are specific to the target sequence, PCR amplification with high fidelity Taq DNA polymerase, DpnI digestion to eliminate the methylated template DNA, transformation into *E. coli* DH5α cells and screening to find the desired mutation. Sequencing of mutated plasmids was done to confirm the mutation. Three mutated constructs were produced as a result of repeating this process for each of the three desired mutations. The sequences of the mutagenic forward and reverse primers for Clone 1 and Clone 2 were 5′- TCTTATGGCAGTATTGGGAGGAAATGAAAACCC-3′ (FP) and 5′-AATACTGCCATAAGATATGCAGCAACGTATTTC-3′ (RP) and 5′-AAAGAGTGCACATGAATTAATTACTGATGGATT-3′ (FP) and 5′- TCAT GTGCACTCTTTCCTTTTAATGAATCAAT-3′ (RP) respectively. To introduce double mutation at the 12th and 53rd position to change the codon: Cysteine (TGC) to Alanine (GCA) and Cysteine (TGT) to Alanine (GCA) respectively, we used primers for Clone 1 on the Clone 2 as DNA template.

Cloning expression and purification of recombinant PfP2, PfP2C12A, PfP2C53A, PfP2C12A +C53A and Plasmodium P1 protein

P2 gene from *Plasmodium falciparum* 3D7 (plasmodb gene ID:PF3D7_0309600) genome was amplified using forward primer 5′-CCCC**GAATTC**ATGGCTATGAAATACGTTGCTG-3′ and reverse primer 5′-GGGG**CTCGAG**TTAACCAAATAAGGAAAATCCTAAGTC-3′. PCR amplified P2 gene and pET28a(+) expression vector were restricted digested using EcoRI and XhoI and the P2 gene was cloned in pET28a(+). Similarly, all mutant versions, P2C12A/P2C53A/P2C12A + PC53A were cloned in pET28a(+) for its expression. Transformed colonies in kanamycin LB agar plate were checked for cloned genes using PCR. The PfP2/PfP2C12A/PfP2C53A/PfP2C12A + C53A were expressed in the *E.coli* BL21 (DE3). Cells transformed with pET-28a(+) vector carrying the encoding gene with 6X His tags at both N′ and C′ terminals. The overnight grown bacterial seed culture, obtained after inoculating 250μL of the glycerol stock along with 25μL of kanamycin (50 mg/ml stock) in 25 mL fresh LB broth, served to be the seed culture for large scale growth at 37°C in 500 mL LB. The cultures reaching OD~ 0.6 were induced with 1mM IPTG and grown till 3.5 h at 37°C. To carry out rec. PfP2 purification, the cell pellets were resuspended in the prepared cell lysis buffer (0.1% Triton X-, 20 mM Tris, 100 mM NaCl) with protease inhibitor for 30 min followed by sonication in ice-cold water for 40 min. The supernatant obtained after the centrifugation of the lysate at 11000 xg for 25 min at 4°C was subjected to 2-3h binding with Hi-bind Ni-NTA agarose beads. The beads were washed 4–5 times with wash buffer (20mM Tris, 100mM NaCl, 25mM Imidazole, pH-7.4) and the His-tagged P2/P2C12A/P2C53A/P2C12A+C53A were finally eluted with elution buffer (20mM Tris, 100mM NaCl and 200mM Imidazole, pH-7.4) and protease inhibitor. The protein concentration was measured using BCA Protein Assay Kit. Recombinant Plasmodium P1 (PfP1) protein was prepared as described in Das et al.[26] Briefly, PfP1 gene was amplified from cDNA using PfP1 FP: 5′-CCCC**GAATTC**ATGGCAT CAATTCCAGCATC-3′ and PfP1 RP: 5′-GGGG**CTCGAG**ACCAAATAAGGAGAAACC-3′. GST tagged PfP1 construct was made by cloning PfP1 gene in between EcoRI and XhoI sites in pGEX-4T3 vector. GST-PfP1 construct was transformed in BL21 DE3 *E. coli* cells for recombinant expression and subsequent purification. Sequence of nucleotides of all cloned genes were confirmed by DNA sequencing.

Urea SDS-PAGE

4M urea was added in resolving and stacking gel. Additionally, 4M urea was also mixed with sample loading dye and in the running buffer. Gel was run like SDS-PAGE and stained with Coomassie R-250.

Treatment of rec. PfP2 with LAFS

4 mg of Albumax was dissolved in 1xPBS (pH 7.4) and passed through a 5 kDa membrane filter (compressed nitro-cellulose) cutoff (Millipore). The cutoff filter was then centrifuged at 1500 xg for 45 min at 4°C. 500μL of the **L**ower **A**lbumax **F**raction **S**olution (LAFS) was obtained at the bottom of cutoff and was treated with 0.5 μg of rec. PfP2 and incubated for 3h at 37°C. The LAFS treated rec. PfP2 sample was purified after binding with Ni-NTA beads for 2h followed by elution of the sample with 20mM Tris-HCl (pH 7.4), 100mM NaCl and 200 mM imidazole buffer. The elute was confirmed to be a pure tetramer in Native PAGE. The confirmed LAFS treated rec. PfP2 tetramer was subjected for various biochemical and biophysical experimentations.

LC-MS of not reduced, not Iodoacetamide (IAA) treated in-gel trypsin digested LAFS treated recombinant PfP2 tetramer

To perform LC-MS to detect serum components, albumax (4 mg) was mixed with 1 mL 1x PBS and the solution was passed through a 5 kD membrane cutoff and centrifuged at 1500 xg for 3h. LAFS obtained at the bottom of the cutoff tube was collected. 2μg of rec. PfP2 was mixed with 500μL of LAFS and incubated for 3h at 37°C with occasional vortexing to facilitate binding. 200 μL of Ni NTA beads was incubated with rec. PfP2+LAFS for 2h at 37°C. Beads were washed and P2 was eluted with elution Buffer. LAFS-treated P2 tetramers were separated in 12% non-reducing, non boiling SDS PAGE. The tetramer band was excised and subjected to destaining using a destaining solution (80 mg of ammonium Bicarbonate (NH_4HCO_3) and 20 mL of Acetonitrile and 20 mL of ultrapure sterile water). Destained gel pieces were dried completely and subjected to trypsin digestion. 50 μL of Trypsin (1μg/100μL) was added to each of the bands and digested overnight at 4°C. The entire trypsin solution was removed and each of the gel pieces was chopped up. 10 μL of 1% TFA was added and incubated for 5 min to stop further digestion by trypsin. After removing the 1% TFA, the samples were further resuspended in 50μL of 0.5% TFA in 5% Acetonitrile. Peptides were further cleaned by C18 resin columns. Cleanup and elution of peptides using C18 column was performed as per the

company protocols. Finally, peptides were eluted in 0.1% TFA in 70% ACN. Precautions were taken to ensure that there was no keratin contamination while handling and processing the samples. ACN and TFA were mass spec grade from J.T.Baker. Analysis was done using XEVO-G2-XS QTOF by Waters.

Parasite membrane preparation

The parasite pellet was resuspended in 1x PBS with 0.1% Triton X-100 and sonicated in ice-cold water. Parasite lysate was centrifuged at 20,000 xg at 4°C for 30 min. The supernatant was collected and the pellet was washed once with 1x PBS. Thereafter, the pellet was resuspended in 1M Na_2CO_3 (pH-10.5) and incubated in ice for 1h with intermittent vortexing followed by centrifugation at 50,000 xg at 4°C for 1h. Carbonate supernatant was collected and the pellet was washed twice with 1x PBS and centrifuged again at 50,000 xg at 4°C for 1h. Now the pellet was treated with 1X SDS loading buffer with reducing agent and boiled. Samples were then centrifuged at 20,000 xg for 45 min and the supernatant was loaded in SDS-PAGE for protein separation and western blotting using various antibodies.

Electron spray ionization (ESI) MS/MS

SDS-PAGE separated parasite membrane proteins (from 180 kDa to 10 kDa) or LAFS-treated recombinant PfP2 tetramer was processed as an unstained gel block/Coomassie-stained gel band. Gel pieces were washed with 100 mM ammonium bicarbonate at 37°C for 15 min followed by washings with 50% Acetonitrile (ACN) in 100 mM ammonium bicarbonate (buffer A) for 15 min at 37°C, until the gel pieces were completely destained. 20 mM DTT in 100 mM ammonium bicarbonate was added and incubated at 60°C for 30 min. Gel pieces were then incubated in 50 mM Iodoacetamide prepared in 100 mM ammonium bicarbonate at room temperature for 45 min in the dark, followed by washing with100 mM ammonium bicarbonate and twice with buffer A. Digestion was set up by the addition of trypsin (0.2 μg/μl) in 100 mM ammonium bicarbonate to as trypsin: protein ratio 1:20; incubated at 37°C for 10h. The supernatant was collected and peptides were extracted in three stages by washing once with 50 mM ammonium bicarbonate and twice with 10% formic acid in 50% ACN. All the extracts were pooled and dried under a vacuum. To desalt the peptide preparation, C18 spin columns were used. Briefly, C18 resin was activated using 200 μL of buffer A, and centrifuged. Resins were equilibrated with 200 μL of 5% ACN, and 0.5% formic acid (buffer B), and centrifuged. This was repeated 3 times. Vacuum-dried samples were dissolved in 200 μL of sample buffer containing 2% formic acid in 20% ACN. Samples were loaded onto the resins and subsequently centrifuged to get the supernatant. This process was repeated 4 times to ensure maximum peptide binding to the resin. The column was washed twice with 200 μL of buffer B. Peptides were eluted using 50 μL 70% ACN. The samples were dried completely under vacuum and suspended in 10 μL of 5% ACN in 0.05% formic acid, before MS/MS analysis using ESI MS/MS in LTQ ORBITRAP XL, Thermo Scientific.

Isothermal Titration Calorimetry (ITC)

5 μM rec.P2/P2C12A/P2C53A/P2C12A + P2C53A were prepared in buffer (20mM Tris, 100mM NaCl) and 90 μM of 2 synthetic fatty acids (FA), PA: Palmitic acid and OA: Oleic acid were prepared in the same buffer. P2 protein was taken in the cell and the ligand (FA) was taken in the syringe. After every 3 min, 10μL of the ligand (FA) was injected into the P2 containing cell under adiabatic condition and heat change due to P2 and FA interaction was recorded. Total 28 injections were made into the cell to assess the saturation of interaction through the changes in heat release/absorbed. As a buffer control, ligand (FA) was injected in only buffer containing cell. ITC was done using MicroCal VP-ITC and data was processed using MicroCal LLC ITC data processing software.

Atomic Force Microscopy (AFM)

rec. PfP2 tetramer/Palmitic acid treated rec. PfP2 tetramer were subjected to Atomic Force Microscopy. 1 μg of rec. PfP2/Palmitic acid treated rec. PfP2 tetramer was firstly diluted 4000x in sterile filtered (0.22 μm membrane filter, Millipore) Milli-Q water to adjust the final concentrations of buffer salts in nanomolar range. 6 μL from the diluted sample was placed at the center of the mica sheet and air-dried in a close cabinet (parafilm wrapped Petri dish). The prepared samples were observed under AFM using 9 μm scanner and cantilever oscillated in Acoustic AC mode. The 2D images were visualized in PicoView 2.0 software, Model 5500, Make-Agilent Technologies.

Import of NBD-Palmitic acid

Synchronized *P. falciparum* 3D7, PfP2–HA transgenic parasite, Chloroquine resistant K1 strain and Artemisinin resistant C580Y strain parasites at trophozoite stage (PMI 26–30 h) were treated with pre-immune sera (400 ng/ul) or anti-P2 Antibody (400 ng/ul) at 37°C for 2 h. PfP2-HA transgenic parasites were treated with/without 3mM GlcN before import assay. After antibody treatment, parasites were incubated with 10μM of NBD-Palmitic acid in phenol red free culture media under the downregulation of PfP2 protein in the parasites or in the presence of pre-immune sera or anti-P2 Antibody (400 ng/ul) at 37°C for 2 h maintaining gas condition. After incubation, NBD-Palmitic acid and antibodies were washed off with phenol red free culture media 3–4 times and then incubated with DAPI (0.1 μg/mL) for 10 min. After final wash, parasites were imaged using Leica confocal microscope and images were processed using ImageJ software. For rescue experiment, after initial anti-PfP2 antibody treatment, antibody was washed off and then the parasites were incubated with 10μM of NBD-Palmitic acid at 37°C for 2 h with maintained gas condition.

During Live cell imaging, synchronized parasites at trophozoite stage (PMI 26–30 h), were first treated with Hoechst 33342 (1 μg/mL) 15 min followed by washing with phenol red free culture media 2–3 times. Parasites were resuspended in phenol red free culture media and layered

on a glass bottom Petri dish pre-coated with Concanavalin A (5 mg/ml). After 1h of infected RBCs attachment, gently unattached RBCs were washed off to achieve a monolayer. 10μM of NBD-Palmitic acid in phenol red free culture media was added in the Petri dish to support parasite growth and image the import of NBD-Palmitic acid in real time. Time laps images after every 15 min were captured, processed and assembled to a movie using ImageJ software.

Flow cytometry of live infected RBCs to assess import of NBD-Palmitic acid

P. falciparum 3D7 infected erythrocytes were synchronized to achieve 4–5% trophozoite stage parasites. Parasites were treated with anti-PfP2 Antibody (400 ng/ul) or pre-immune sera (400 ng/ul) at 37°C for 2 h. After the treatment, parasites were incubated with 10μM NBD-Palmitic acid in phenol red-free culture media in the presence of anti-PfP2 Antibody (400 ng/ul) or pre-immune sera for 2 h at 37°C. After the incubation, parasites were washed 2–3 times with phenol red free culture media and treated with DAPI (0.1 μg/mL) for 10 min. Up to 0.5 million cells were assessed for the import of NBD-Palmitic acid using LSR Fortessa (BD Biosciences, USA) and analyzed by FLOWJO software.

Triglyceride (TG) quantification

P. falciparum 3D7, Chloroquine resistant K1 strain, and Artemisinin-resistant C580Y strain culture were synchronized and treated (PMI 10-12h) with various treatments such as Furosemide (20μM), taxol (0.5 μM) and anti-P2-Abs (400 ng/μL), Orlistat (10μM) and pre-immune serum (400 ng/μL) in 6 well plates. Each treatment was done in triplicate. After 24–26 h of incubation, parasites were treated with 0.1% saponin in 1x PBS for 10 min. The parasite pellet was washed at least two times with 1x PBS or until there was no visible trace of hemoglobin in the supernatant. The parasite pellets were lysed in 1x PBS (pH 7.4) with brief sonication in ice. The lysate was boiled at 100°C for 5 min and centrifuged at 11000 xg at 4°C for 10 min and the supernatant was used for the triglyceride (TG) quantification. Triglyceride quantification was performed according to the manufacturer's protocol. Briefly, all treated samples and standards were treated with lipase and incubated for 20 min at room temperature, followed by master mix treatment for 60 min (dark incubation) at room temperature. Optical density (OD) was measured at 570 nm using a microplate reader and plotted a standard curve after the subtraction of blank control value. Concentrations of TG in the sample lysates were determined using the standard curve.

QUANTIFICATION AND STATISTICAL ANALYSIS

Quantification and statistical calculation were done and plotted as mean ± S.E.M. Significance was calculated by unpaired Student's t test or one-way ANOVA. Significance was considered at $*p < 0.05$, $**p < 0.01$, $***p < 0.001$. Not significant was denoted as P=NS. N represents biological replicates. All quantitative experiments were repeated at least three times or more as indicated.